G104051

ABSTRACT

MEMBRANE-BOUND ATP-ASE ACTIVITY, INTRACELLULAR pH AND MEMBRANE POTENTIAL OF MYCOPLASMAS

PART I: LIPID AND TEMPERATURE DEPENDENCE OF MEMBRANE-BOUND ATP-ASE ACTIVITY OF ACHOLEPLASMA LAIDLAWII

PART II: INTRACELLULAR pH AND MEMBRANE POTENTIAL OF THERMOPLASMA ACIDOPHILA

By

Jean-Cheui Hsung

The activity of membrane-bound enzymes may depend upon the presence of lipids, and protein-lipid interaction may play an important role in enzyme function. Thus, the effects of fatty acyl chain length on the membrane physical states and membrane-bound ATPase activity of Acholeplasma ladlawii were investigated.

Three membrane preparations from cells were obtained by supplementing the growth media with either arachidic ($C_{20:0}$), oleic ($C_{18:1}$) or lauric ($C_{12:0}$) acid. The cells grown with arachidic or oleic acid supplementation yielded membrane lipids enriched with arachidoyl or oleoyl groups respectively. Those supplemented with lauric acid yielded membrane lipids enriched with myristoyl and palmitoyl groups.

The membrane-bound ATPase activity of membrane preparations were measured in the temperature range from 15 ^{o}C to 45 ^{o}C. Arrhenius plots of the ATPase activity of membranes enriched with either arachidoyl

or myristoyl-palmitoyl groups exhibited a pronounced discontinuity in slope around 26 ^{o}C - 30 ^{o}C. On the other hand, the Arrhenius plots of the ATPase activity of membranes enriched with oleoyl groups showed no breaking point in the temperature range from 15 ^{o}C to 45 ^{o}C.

The membrane lipid fluidity was measured with a nitroxyl stearic acid spin label. At the growth temperature (37 ^{o}C) the membrane lipid fluidity of all three kinds of enriched membranes was virtually identical. For membranes enriched with saturated acyl chains, a plot of the EPR anisotropy parameter $2T_{\perp}$, versus the reciprocal of temperature showed a biphasic profile with a discontinuity in slope around 26 ^{o}C - 30 ^{o}C. For oleoyl group enriched membranes this plot yields only a straight line, without a breaking point in the temperature range from 15 ^{o}C - 45 ^{o}C. Thus, the Arrhenius plots of the ATPase activity and $2T_{\parallel}$ correlated well. This indicates that the physical state of membrane lipids does play a role in determining the activation energy of the membrane bound ATPase. This enzyme is probably localized in the more fluid regions of the membrane where the fatty acid spin label is also preferentially located.

* * * * *

Thermoplasma acidophila, a mycoplasma-like organism, was grown at pH 2, at 56 ^{o}C. This is a prokaryotic micro-organism devoid of a cell wall bounded by a single membrane without any intracellular membrane bound organelles. The intracellular pH was measured on the basis of the distribution of a radioactive weak organic acid, 5,5-dimethyl-2,4-oxazolidine-dione, "across" the plasma membrane. It was found that the

intracellular pH lies in the neutral range from pH 6.4 to 6.9. This agrees with a direct pH measurement of the cavitation fluid and indirect conjecture from enzyme profiles.

The cell can maintain a huge pH gradient when subjected to heat or metabolic inhibitors. The membrane potential of the cell was measured by the distribution of a radioactive anion SCN^- which dissociates almost completely at pH 2. The membrane potential is 120 mV positive inside, and is independent of the presence of metabolic inhibitors. The membrane potential decreased linearly with the external pH. The membrane potential virtually diminished when the external pH was raised to 6.

The surface charge density and the zeta-potential was estimated by microscopic electrophoresis. The cells moved towards the positive electrode. The mobility remained constant from pH 2-5, and increased for $pH > 6$. The mobility decreased dramatically with increased external Ca^{++} concentration at pH 6, and only slightly depended on Ca^{++} ion concentration at pH 2. At pH 2 and an ionic strength similar to that of the growth medium, the zeta-potential was about 8 mV, negative relative to the bulk medium; the surface charge density was -1360 esu/cm^2 which corresponds to one elementary charge per 3500 A^2.

The compatibility of the observed data with the chemiosmotic theory of energy coupling is discussed.

MEMBRANE-BOUND ATP-ASE ACTIVITY, INTRACELLULAR pH AND MEMBRANE POTENTIAL OF MYCOPLASMAS

PART ONE: LIPID AND TEMPERATURE DEPENDENCE OF MEMBRANE-BOUND ATP-ASE ACTIVITY OF *ACHOLEPLASMA LAIDLAWII*

PART TWO: INTRACELLULAR pH AND MEMBRANE POTENTIAL OF *THERMOPLASMA ACIDOPHILA*

By

Jean-Cheui Hsung

A DISSERTATION

Submitted to
Michigan State University
in partial fulfillment of the requirements
for the degree of

DOCTOR OF PHILOSOPHY

Department of Biophysics

1977

DEDICATION

To my parents, brother and sisters

and

Hwai-chyi

ACKNOWLEDGMENT

The author wishes to express his sincere appreciation to Dr. Alfred Haug for his guidance, encouragement and criticism , as both major professor and friend, during the course of this study. Special thanks are extended to Drs. H.Ti. Tien, Michael Jost, Estelle McGroarty and Ashraf El-Bayoumi for serving as guidance committee members.

Very special thanks go to Hwai-chyi for her love, faith and encouragement during my graduate years.

The author also wish to thank Dr. Anton Lang for enabling him to carry out this research in the MSU/ERDA Plant Research Laboratory. This work was supported by United States ERDA contract no. EY-76-C-02-1338 *000

LIST

LIST

ORGA

CHAP

PART

CHAP

TABLE OF CONTENTS

LIST OF TABLES

LIST OF FIGURES

Figu

7.

8.

9.

10.

11.

12

13

14

15

1

ORGANIZATION OF DISSERTATION

A General Introduction is in Chapter I. The main body of this dissertation consists of two parts. Part One, (Chapter II) deals with Lipid and Temperature Dependence of Membrane-Bound ATPase Activity of Acholeplasma laidlawii. Part Two, (Chapter III and IV) deals with Intracellular pH and Membrane Potential of Thermoplasma acidophila. References are combined at the end of the dissertation.

L

they a

differ

aperio

crysta

inform

and t

the o

therm

surro

with

ing,

the

mech

but

synt

orga

CHAPTER I

GENERAL INTRODUCTION

Living systems and non-living systems have one thing in common, they all consist of matter. But their structures and functions are different, the living systems consist of what Schrödinger called the aperiodic crystal, and the non-living systems consist of the periodic crystal if there is a crystal structure at all. According to their information content living systems tend to maintain an organization, and to keep the local entropy low within the biological systems; on the other hand, non-living systems tend to increase their entropy as thermodynamic equilibrium approaches (1).

Living cells have to keep themselves separated from their surroundings; at the same time they must be in dynamic interaction with their environment. At the interface of the cell and its surrounding, there is the cell membrane.

Biological membranes not only play an active role in regulating the internal environment of the cell, selecting substrates through the mechanism of facilitated diffusion or active transport (for review 2-4); but are also important in energy transduction (5,6) and macromolecular synthesis (7). They may also play an important role in protecting the organism when under environmental stress (8).

vari

rent

unkn

rose

(3,1

Gorc

cyte

foun

assu

arra

secu

grou

eith

phot

Gren

mode

Sur-

seve

as r

Ques

rath

Outs

evi

Biological membranes consist mainly of lipids and proteins in various ratios, and some polysaccharides. The exact molecular arrangement of these components in three-dimensional structure is still unknown, but several membrane models have been proposed. Two important models will be reviewed.

The classical lipid bilayer model proposed by Davson-Danielli (9,10) was based on thermodynamic considerations and experiments of Gorter and Grendel (11). They prepared a lipid extract from erythrocytes, and spread it as a monomolecular film on a Langmuir trough, and found that the film area was approximately twice the total surface area assumed for the total red cells used. In this model, lipids are arranged in two layers, the nonpolar sidechains of the lipids are sequestered together and shielded from water, whereas the polar head groups of the lipids are in direct contact with the aqueous phase on either side of the membrane, and therefore, maximize both the hydrophobic and hydrophilic interactions. Although the original Gorter-Grendel experiment may have several mutual "offsetting errors" (for modern review, see 12), the basic concept of the lipid bilayer has survived for all these years. It has induced the development of several artificial systems such as that of the Black Lipid Membranes, as model systems for membrane research (13,14).

The main shortcoming of the Davson-Danielli model is not the question of whether or not the lipids are arranged in a bilayer, but rather the position of the proteins. Originally the proteins were put outside the bilayer, in globular or extended β-form.

Based on thermodynamic considerations and some experimental evidences, Singer-Nicolson proposed the fluid-mosaic model (15,16).

A sketch of the model is presented in Figure 1 (16). "In this model, the proteins that are integral to the membrane are a heterogeneous set of globular molecules, each arranged in an amphipathic structure, that is, with the ionic and highly polar groups protruding from the membrane into the aqueous phase, and the nonpolar groups largely buried in the hydrophobic interior of the membrane. These globular molecules are partially embedded in a matrix of phospholipids. The bulk of the phospholipids is organized as a discontinuous, fluid bilayer, although a small fraction of the lipid may interact specifically with the membrane proteins. The fluid mosaic structure is therefore formally analogous to a two-dimensional oriented solution of integral proteins (or lipoproteins) in the viscous phospholipid bilayer solvent."

This model is strongly supported by the following experimental evidence. In freeze-etch electron microscopic studies, the proteins can be visualized as intercalated particles (17,18). Enzymatic iodination of biological membranes by lactoperoxidase has also shown that some proteins can be labelled from both sides of the membrane, which indicates that these kinds of protein span the membrane (19,20).

One feature of the fluid mosaic model is the dynamic character of the proteins and lipids in the membrane. The model suggests that at physiological conditions, the membrane is in a liquid-crystal fluid state and the proteins can laterally diffuse in the two dimensional lipid solvent.

To investigate the physical states of the lipids in the biological membrane, several physical techniques have been used (for recent review, see reference 21,22). They can be broadly divided into two categories.

Figure 1. The fluid mosaic model of biological membrane; schematic three-dimensional and cross-sectional views. The solid bodies with stippled surfaces represent the globular integral proteins, which at long range are randomly distributed in the plane of the membrane. At short range, some may form specific aggregates. Lipids form a matrix.

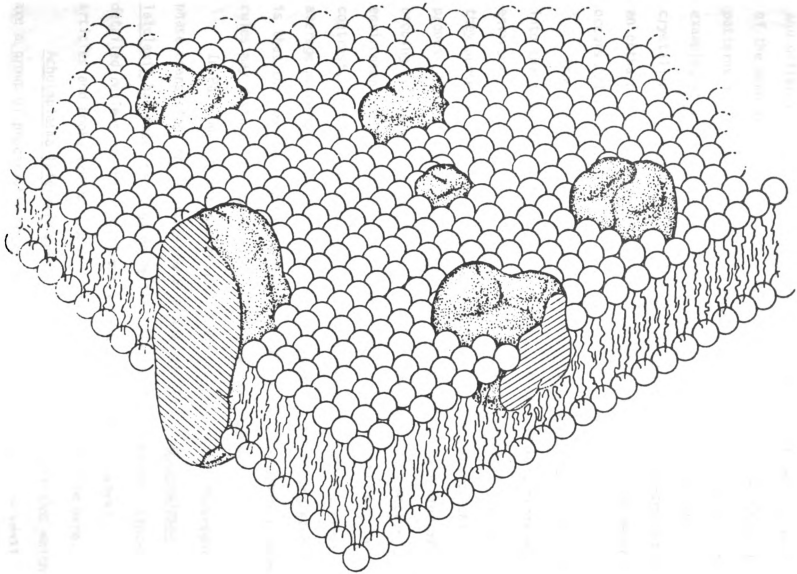

Figure 1

The techniques in the first category, such as X-ray diffraction and differential scanning calorimetry, measure some intrinsic characters of the membrane. X-ray experiments measure the change of diffraction patterns in dependence of physical states of the membrane lipids, for example, at a transition from a thermotropic gel (order) to liquid crystalline (disorder) (23). Differential scanning calorimetry measures an enthalpy change when an endothermic phase transition of the membrane occurs (24).

Those in the second category involve sending "reporter" molecules into the membrane. The reporter molecules are sensitive to their micro-environment, so they will report any change in the physical states as they perceive. The commonly used "reporters" include fluorescent probes (25) and spin labels (26,27). The advantage of this kind of probing technique is that it can provide information of the micro-environment such as microviscosity or fluidity very sensitively, in contrast, differential scanning calorimetry can only measure a gross average property of the membrane. The disadvantage of probing studies is that the news breaker may become news maker, i.e., the probing molecules may disturb the system which they intend to measure.

In Part One of this dissertation, the influence of thermotropic phase transitions on membrane-bound ATPase activity of Acholeplasma laidlawii has been investigated by the spin labelling method. Since detailed reviews on this organism have been published in several articles and books (28-30), only a simple summary is presented here.

Acholeplasma laidlawii belongs to the order Mycoplasmatales which are a group of procaryotic micro-organisms. They are generally small

in s

a si

Ignc

ster

stuc

stru

75-1

arou

part

exog

mem

sol

rea

str

are

tio

dif

tio

con

or

in size (0.2 to few μm in diameter), devoid of a cell wall, bounded by a simple membrane without any intracellular membrane bound organelles. Acholeplasma laidlawii differs from other mycoplasmas by requiring no sterol for growth.

Acholeplasma laidlawii has been the subject of many membrane studies in recent years. Electron microscopy reveals a "unit membrane" structure both in cells and in isolated membranes with a thickness of 75-100 Å. The lipids are mainly phospholipids, glycolipids and varing amounts of carotenoids. The lipids can be highly enriched with a particular fatty acyl group when the corresponding fatty acid is supplied exogeneously. Polyacrylamide gel electrophoresis of the solubilized membrane exhibits at least 20 to 30 bands (31,32). It is possible to solubilize the membrane into small subunits by detergents, and form a reaggregated membrane after removing the detergents. Lipid bilayer structure resumes in the "reaggregated membrane". However, the proteins are incorrectly reassembled in these membranes (33,34). Phase transitions of the hydrocarbon chains in the bilayer have been detected with differential thermal calorimetry, EPR spin labelling, and X-ray diffraction techniques.

* * * * *

One of the most important questions in biology is how energy is converted from one form into another one. How energy, gained from light or food stuff, can be employed to carry out biological functions.

For mitochondria or micro-organisms, this question would be: how does the energy from the respiratory electron transport chain couple to

the ATP synthesis and other biological functions, such as active transport of cations? Currently, there are three theories of energy coupling: (1) Chemical intermediate theory (35,36), (2) Chemiosmotic theory (37-40) and (3) Mechanoconformational coupling theory (41-43).

The chemical intermediate theory is the oldest of the three. A modified version of the original form proposed by E. C. Slater (35) put the scheme of this hypothesis as follows (44):

$$A_{ired} + B_{iox} \rightleftharpoons A_{iox}\sim I + B_{ired} \qquad (1)$$

$$A_{iox}\sim I + X \rightleftharpoons A_{iox} + X\sim I \qquad (2)$$

$$X\sim I + P_i \rightleftharpoons X\sim P + I \qquad (3)$$

$$X\sim P + ADP \rightleftharpoons X + ATP \qquad (4)$$

Here A_i, B_i are adjacent respiratory carriers at a given coupling site and X and I are energy-transfer carriers common to all three sites. Equation (1) shows the "energy-coupling reaction" and the other equations represent "energy-transfer reactions".

The chemical hypothesis has many virtues, but it is somewhat unfortunate that no high energy intermediate, phosphorylated or non-phosphorylated, of mitochondrial respiratory chain phosphorylation has ever been discovered (45,46).

A merit of the chemiosmotic theory as a scientific hypothesis lies in the fact that it can be subjected to crucial experimental tests. Even the validity of the chemiosmotic theory of energy coupling has not yet been accepted <u>in total</u> by the scientific community, it is universally agreed that it is the most influential theory in energy coupling. Since Mitchell proposed the hypothesis in 1961 (37), and in more elaborated

form

to di

prim

resp

cyto

has

forw

is a

mem

able

elec

thro

the

to t

into

tran

"pr

* B
c
m
h
e
c

form afterwards (38-40), it has triggered extensive research trying to disprove or verify this hypothesis.

The mechanoconformational coupling theory proposed that the primary energy-conservation process is a conformational change in a respiratory protein - a flavoprotein, an iron-sulfur protein or a cytochrome - and this energy may be utilized to make ATP. This theory has often been critisized for its vagueness and difficulty in putting forward for experimental test (53).

The basic feature of the chemiosmotic theory of energy coupling is as follows (A sketch is presented in Figure 2):

(1) The coupling membrane of the inner mitochondrion or plasma membrane of micro-organisms is permeable to water and virtually impermeable to protons and most other ions, and therefore is of very low electrical conductivity.

(2) The oxidoreductions, causing hydrogen and electron transport through the respiratory chain in the forward direction, result also in the translocation of protons from the inner phase of the mitochondrion to the outer phase. The respiratory chain is supposed to be folded into "oxidoreduction loops" corresponding to the three coupling sites.

(3) The respiration-driven proton translocation generates a transmembrane electric potential and/or pH difference, together called "proton motive force". In electric units, a 270 mV* proton motive

* Based on the high (ATP)/(ADP)x(Pi) ratio observed in state 4 mitochondria, the opponents of Mitchell's hypothesis have put the proton motive force required for ATP synthesis in state 4 mitochondria as high as 370 mV, if the P:2e ratio is assumed to be equal to 2 for each coupling site of respiratory chain. This statement has been considered by some as not to be rigorously substantiated because of the complication of the existence of ATP, ADP porters in the inner mitochondria membrane (54,55,66)

Figure 2. Chemiosmotic hypothesis: extrusion of protons by the respiratory chain, generation of ΔpH and $\Delta\psi$, and the poising of ATPase by the proton-motive force. (From reference 53).

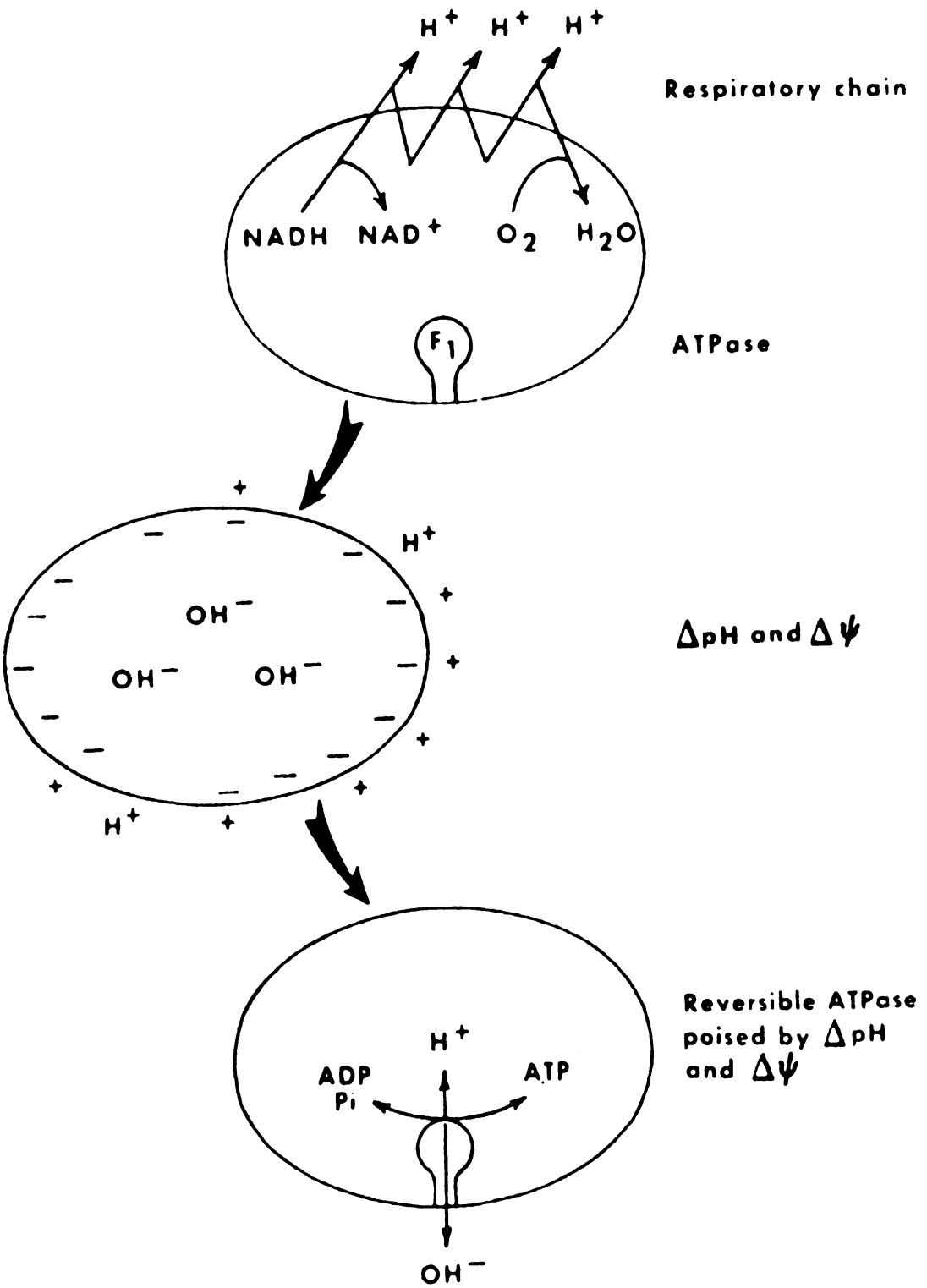
H+ H+ H+
Respiratory chain
NADH NAD+ O2 H2O
F1
ATPase
H+
OH−
OH− OH−
ΔpH and Δψ
H+
ADP
Pi
H+
ATP
Reversible ATPase
poised by ΔpH
and Δψ
OH−

Figure 2

force is needed for ATP synthesis, if H^+/P ratio is 2.

(4) There exists a membrane-bound reversible ATPase which can transport protons from the inside of the mitochondrion to the outside. Protons flow back from the outside to the inside of the mitochondrion, i.e., down their electrochemical gradient, trigger ATP synthesis.

(5) For this coupling mechanism to function, two corollaries must hold: (i) A closed membrane is necessarily required for energy coupling. (ii) To compensate for what Mitchell called "backlash", exchange transport systems should exist, in which cations may antiport and anions may symport with protons, or with each other.

The fundamental difference between the chemiosmotic theory and the conventional ones is that in Mitchell's hypothesis, H^+ ions separated by an osmotically intact membrane are the coupling agents. Both the membrane potential, and the H^+ ion chemical potential difference between two aqueous phases separated by the coupling membrane, are properties belonging to the whole membrane phase. It does not require "direct microscopic contact" of the redox chain with the reversible ATPase in physical space. In contrast, the chemical, conformational, or the modified "electromechanochemical" coupling developed by Green et. al (47-49) all require a direct contact of the two. Thus, it would be expected that normal biochemical fractionation methods should provide evidence for well defined structural associations and functional interrelationships between redox and the ATPase components. This is contrary to the experimental finding of biochemists despite forty years of diligent searching (51).

Although some controversial points still remain, (for unsympathetic reviews 36, 47-50), a vast amount of evidence has been accumulated in recent years in support of the main feature of the chemiosmotic theory (for review, 44, 51-55). Some of them are summarized below:

(1) In both mitochondria and submitochondrial particles, oxygen pulse and ATP hydrolysis do cause vectorial proton translocations in the right stoichiometry (56-59). Two proton pumps have been isolated and reconstituted in liposome systems and are found to be intrinsic expressions of the redox chains and the reversible ATPase systems. The two pumps are apparently separate. They do not share any chemical component in the membrane but can be shown to be energetically coupled one to another through cyclic proton current (60-63). Kinetically, they are fast enough to mediate between respiration and phosphorylation (59, 64).

(2) There is no doubt that there exist energy-linked exchange diffusion systems of cations and anions with proton translocation (65, 66). But which one is directly linked to metabolism is a controversial point. Evidence accumulated in recent years seems to indicate that it is the proton current which is primarily linked to metabolism (54,55). The inhibitors of cation transport have no direct effect on the proton pump (59,67). Kinetic analysis shows that both the redox and the hydrolytic proton translocations are immediate expressions of the oxidation and reduction reactions of the respiratory chain and the hydrolytic reaction of ATPase system respectively. They do not depend upon the build-up of labile energy-rich chemical intermediates (59,68, 69). The transmembrane electric potential thus generated causes

electrophoretic migration across the membrane of any permeant cations or anions aspecifically (52,67,68).

(3) The coupling membranes are not readily permeable to protons (70,71). The classical uncouplers of oxidative phosphorylation such as 2,4-nitrophenol function as proton conducting agents specifically equilibrating the electrochemical potential of H^+ ions across the coupling membrane (72). The study of a number of structurally dissimilar compounds has revealed a linear relationship between their effectiveness as protonphores in artificial phospholipid membranes, and uncouplers in mitochondria (73). Uncouplers do not depress the H^+/O ratio in both intact mitochondria and submitochondrial particles obtained by cavitation (56,74).

(4) Energization of coupling membranes either by redox chain or by ATP hydrolysis can generate a transmembrane electric potential and/or a pH difference irrespective of the formation of high-energy intermediates (54). In state 4 mitochondria, a membrane potential of 230 mV (negative inside), has been observed by measuring the distribution of K^+ in the presence of valinomycin (75) and synthetic organic Skulachev ions, such as phenyl dicarbaundecaborane (PCB^-), and N,N-dibenzyl N,N-dimethyl ammoninum (DDA^+) (76,77). A pH gradient of 0.4 to 0.8 pH units has also been obtained by titrimetric methods or by measuring the distribution of a weak acid (78). The total proton motive force of 270 mV is considered by some as thermodynamically adequate for ATP synthesis (see foot note on page 9).

(5) Energy accumulated in the form of transmembrane electric and osmotic gradients can be utilized for ATP synthesis. In chloroplasts, an artificially imposed pH gradient can induce ATP formation in the dark

with

efflu

mitoc

and

cert

is b

atta

(oli

The

also

loc

chr

rea

mer

che

fo

my

is

a

p

i

t

a

p

w

with electron flow prevented by inhibitors (79). An artificial K^+ efflux, down their electrochemical gradient can cause ATP synthesis in mitochondria (80).

(6) The three-dimensional arrangement of the respiratory chain and ATPase system in the mitochondrial membrane is still far from certain. Some evidence indicates that the inner mitochondrial membrane is both structurally ahd functionally asymmetric. ATPase (F_1) is attached to the matrix side of the inner membrane by the stalk component (oligomycin sensitivity conferring factor) of the ATPase complex (81,82). The active sites of NADH dehydrogenase and succinate dehydrogenase are also located on the matrix side of the membrane. Cytochrome c is located on the outer cytoplasmic side of the membrane (81,83). Cytochrome oxidase appears to be a transmembranous molecule with its oxygen-reaction site located at the matrix side of the inner mitochondrial membrane (84,85). All these aspects are basically consistent with the chemiosmotic hypothesis.

The chemiosmotic hypothesis put the proton in a unique position for biological function. In the second part of this dissertation, a mycoplasma-like organism Thermoplasma acidophila was investigated. It is a procaryotic micro-organism with a single compartment enclosed by a simple plasma membrane. It was first isolated from a coal refuse pile and has an optimal growth at pH 2 and 59 ^{o}C (86). It is interesting to know how this organism can live in such an environment without the protection of a cell wall. Thermoplasma acidophila can not grow at a temperature higher than 62 ^{o}C, which is very close to the high temperature limit found empirically for acidophiles (87). No organism which requires a pH less than 3 and yet can grow at 70 ^{o}C has been

found. Thus, Thermoplasma acidophila represents the edge of the acidophilic, thermophilic frontier at which life may exist.

It becomes both important and interesting to know what is the intracellular pH, the membrane potential of this thermophilic, acidophilic organism. The compatibility of the experimental results from this organisms in extreme environment, will be discussed in terms of the chemiosmotic hypothesis.

PART ONE

LIPID AND TEMPERATURE DEPENDENCE OF MEMBRANE-BOUND ATP-ASE ACTIVITY OF *ACHOLEPLASMA LAIDLAWII*

CHAPTER II

LIPID AND TEMPERATURE DEPENDENCE OF MEMBRANE-BOUND ATP-ASE ACTIVITY OF ACHOLEPLASMA LAIDLAWII

Introduction

The activity of membrane bound enzymes may depend upon the presence of membrane lipids (88,89). Alteration of the membrane lipid composition can be achieved by nutritional supplementation of selected fatty acids for organisms with limited fatty acid biosynthetic capabilities (90,91) or by adjusting the growth temperature of poikilotherms (92). Acholeplasma laidlawii cells have the property that the membrane lipids can be enriched with respect to a selected fatty acid group via proper supplementation of the growth medium (93). Therefore, this organism has been the object of numerous studies to correlate various membrane properties with the acyl group composition.

Previous investigations have demonstrated that Acholeplasma laidlawii cells have a tightly bound membrane ATPase which is Mg^{++} dependent and independent of Na^{+} and K^{+} ions (94). Alteration of the lipid acyl groups by nutritional supplementation and measurement of the ATPase activity from membrane suspensions at various temperatures can determine lipid dependence while avoiding the difficult experimental problem of membrane solubilization, enzyme purification, enzyme stability, and lipid reconstitution. These harsh treatments might

possibly introduce artifacts.

A careful approach was also carried out for Escherichia coli membrane bound enzymes (95,96). In an unsaturated fatty acid auxotroph of Escherichia coli, membrane fatty acyl composition was changed by supplementing the nutrient medium with either cis-vaccenic, oleic, linoleic, linolenic acids or their corresponding trans-unsaturated fatty acids as the sole unsaturated fatty acid.

One class of enzymes, such as acyl-CoA:glycerol 3-phosphate acyltransferase, were inactivated at a rate similar to the rate of phospholipase C hydrolysis of total membrane lipids, and were also characterized by an Arrhenius plot depending on whether the membrane contains cis-unsaturated or trans-unsaturated fatty acids. The other class of enzymes, such as glycerol 3-phosphate dehydrogenase, remained completely active after 95% of their membrane phospholipids had been hydrolyzed by phospholipase C, and their Arrhenius plots were characterized by a linear curve without a breaking point, and identical in slope, independent of membrane fatty acyl composition.

In the case of Acholeplasma laidlawii, strain B, discontinuities in the Arrhenius plots of the ATPase activity occurred at the lower end of the lipid phase transitions, as measured by differential scanning calorimetry. The organism was enriched with saturated or unsaturated fatty acids varying in chain length from 16 to 18 carbon atoms (97).

With respect to the membrane of Acholeplasma cells, structural changes associated with phase transitions in the lipid bilayer portion have been studied with X-ray diffraction (98), electron paramagnetic resonance (99,100), and differential scanning calorimetry (24,97). Recently, freeze fracture studies of membranes demonstrated that the

lipid

aggre

ture

in b

Arrh

the

spin

and

cel

or

of

phy

be

act

ob

Or

(

c

b

t

a

lipid bilayer continuum becomes interrupted by protein particles which aggregate or disperse dependent on fatty acyl composition and temperature (101,102).

The possibility of interpreting the change in activation energy in biological system, revealed in the presence of breaking points in Arrhenius plots, as a phase transition or at least as an indication of the beginning of the fluid-order transition has been discussed (103-105).

In the following studies, electron paramagnetic resonance (EPR) spin labelling methods are used to monitor the membrane lipid fluidity and to detect any possible phase transition. The Acholeplasma laidlawii cells are grown on a nutrient medium supplemented with either oleic acid or saturated fatty acids containing 12 or 20 carbon atoms (106). Because of such a difference in acyl chain length, it is expected that the physico-chemical membrane properties vary distinctively. Attempts will be made to correlate the dependence of the membrane bound ATPase activity on fatty acyl composition and temperature with information obtained from EPR spin labelling experiments.

Material and Methods

Organism and Growth

Acholeplasma laidlawii (oral strain) was a gift from Dr. S. Rottem (The Hebrew University, Jerusalem, Israel). The basal growth medium consisted of 20g Bacto-tryptose (Difco, Detroit, Michigan) which had been lipid extracted (107), 5g D-glucose, 5g sodium acetate, and 5g tris (hydroxymethyl) aminomethane per liter. The pH of the medium was 8.2 to 8.4 without adjustment. Four g/l of bovine plasma albumin fraction V (Armour Pharmaceutical Co., Chicago, Illinois) was charcoal treated to remove fatty acids (108) and then sterilized by Millipore

filtration together with 500 units/ml of penicillin G (Sigma, St. Louis, Missouri). The filtrate was then added to the basal medium. Either arachidic, oleic or lauric acid (5mg/l) was introduced into the growth medium as a 70% aqueous ethanol solution. The final ethanol concentration in the medium never exceeded 0.5%. The cells were originally grown in oleic acid supplemented medium. They could be adapted to supplementation with arachidic or lauric acid after 6-10 daily transfers. The medium was inoculated (1% v/v) with a 24 hour-old cell culture. The cells were grown statically at 37°C, and harvested after 20-24 hours for oleic or arachidic acid supplemented cells and 96 hours for lauric acid supplemented cells (106).

Plasma Membrane Preparation

Cells were harvested at late log phase of growth by centrifugation at 10,000 x g and were washed once in β-buffer, which contains: 1% NaCl, 0.6% tris(hydroxymethyl)aminomethane, and 0.07% (v/v) 2-mercaptoethanol prepared in deionized distilled water and adjusted to pH 7.4 with HCl. (109). To isolate membranes, cells were lysed by squirting washed cells into 1:20 diluted β-buffer, then incubated and stirred gently at room temperature for one hour. After incubation, unlysed cells were removed from the membrane preparation by centrifuging at 3,000 x g for 5 minutes, the supernatant was centrifuged for 30 minutes at 4°C at 37,000 x g, then washed once with 1:20 β-buffer. The pellet was then resuspended in 1:20 β-buffer and adjusted to 1 mg/ml protein concentration and stored at 4°C. The same batch of membrane preparation was divided into three parts, one for ATPase assay (which was always completed within 48 hours), one for lipid fatty acyl composition analysis, and one for spin labelling

experiments.

ATPase Assay

The ATPase assay followed the method of Ruthbun and Betlach (110). Although the ATPase activity of Acholeplasma laidlawii was not dependent on K^+, Na^+, the assay solution always contained 0.1 ml of 10 mM KCl, 0.1 ml of 10 mM NaCl, 0.1 ml of $MgCl_2$, and 0.1 ml of 0.5 mM tris-(hydroxymethyl)aminomethane, HCl (pH7.6), 0.05 ml 20 mM ATP (Sigma, St. Louis, Missouri) plus appropriate amounts of membrane preparation and adjusted with deionized distilled water to a total volume of 1 ml. After incubation for 15 or 45 minutes (dependent on temperature), the reaction was stopped with cold 10% trichloroacetic acid (TCA), and centrifuged at 10,000 rpm (Sorvall GS 34 rotor) for 5 minutes. The supernatant was added to 1 ml 3M sodium acetate-acetic acid (1:1 V/V), the final pH was 4.2. To develop color, 0.1 ml 2% ammonium molybdate and 0.2 ml stannous chloride 1.52 mg/ml was added. The last two reagents were freshly prepared on the day of the experiment. After 15 minutes of incubation, the absorbance at 730 nm was recorded with a Gilford spectrophotometer, model 2400. A blank with ATP and a blank with the membrane preparation were always run in conjunction with the rest of the assays.

All experiments were done in a cold room (4^oC), in water baths maintained at temperatures from 6^oC to 45^oC. The duration of one set of experiments usually lasted from 12 to 18 hours. The enzyme has a half life of 10 days when stored at 4^oC. Therefore, the enzyme will change its activity less than 2% during the period for one set of experiments.

The protein concentration was determined by the method of Lowry et. al. (111).

Fatty Acyl Analysis

Membrane lipids were extracted with chloroform-emthanol (2:1, v/v), washed with salt solution (0.02% $CaCl_2$, 0.017% $MgCl_2$, 0.29% NaCl and 0.37% KCl), and dried under nitrogen according to Folch et. al.(112). Methyl esters of fatty acids were prepared by reacting about 4 mg of lipids in 4 ml of 2% (v/v) concentrated H_2SO_4 in methanol at 40°C for 24 hours. The methyl esters were extracted with hexane and quantitatively analyzed by chromatography on a diethylene glycol succinate column at 190°C. A Hewlett-Packard gas chromatograph, model 402, equipped with a flame ionization detector was employed. The esters were identified by comparison with standards obtained from Applied Science Lab., Inc., State College, Pennsylvania. Relative quantities of fatty acyl composition were measured from the areas under the peaks of the chromatogram.

Solubilization of Membranes

Membrane suspensions (1 mg protein/ml) were treated for one hour at 37°C with an equal volume of 0.1% Triton X-100. The clear solutions were centrifuged for one hour with a Beckman L-65 ultracentrifuge, SW 40 rotor at 38,000 rpm (180,000 x g). ATPase activity was present in the supernatant.

EPR Spectroscopy

Isolated Acholeplasma laidlawii membranes were labelled in vitro with a fatty acid spin label. We used the label 2-(3-carboxypropyl)-4, 4-dimethyl-2-tridecyl-3-oxazolidinyloxyl (abbreviated as: 5NS), or the spin label 2-(10-carboxydecyl)-2-hexyl-4,4-dimethyl-3-oxazolidinyloxyl (abbreviated as: 12NS), (for molecular structure see Figure 3), obtained from Synvar Corporation, Palo Alto, California.

Figure 3. The molecular structure of the spin labels 2-(3-carboxypropyl)-4,4-dimethyl-2-tridecyl-3-oxazolidinyloxyl, 5-nitroxyl stearate, abbreviated as 5NS. 2-(10-carboxydecyl)-2-hexyl-4,4-dimethyl-3-oxazolidinyloxyl, 12-nitroxyl stearate, abbreviated as 12NS.

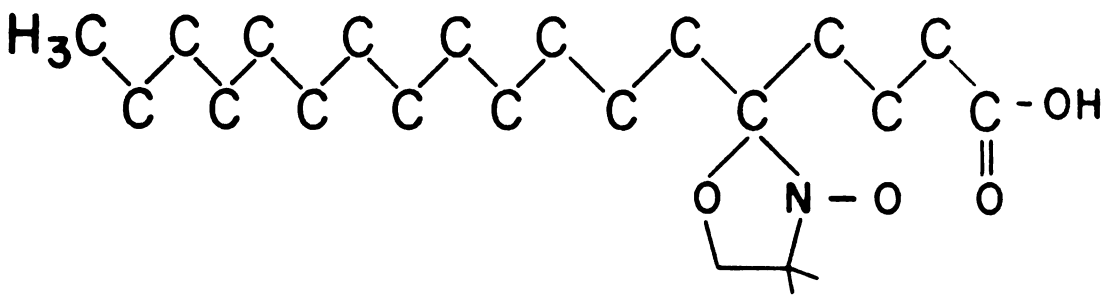

5-nitroxyl stearate: 5 NS

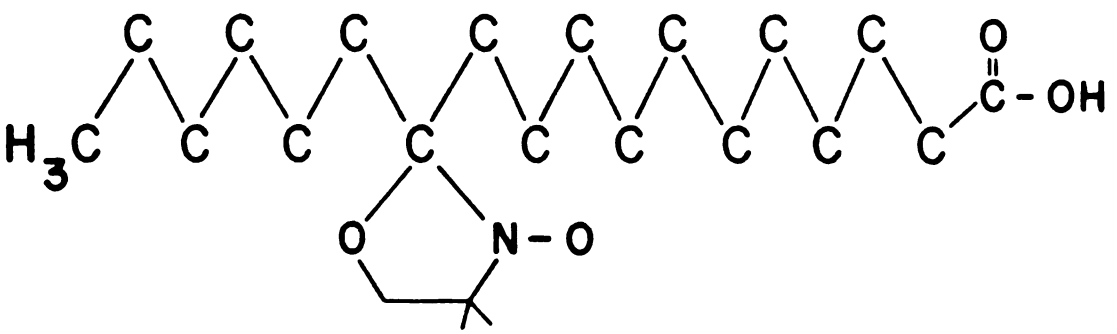

12-nitroxyl stearate: 12 NS

Figure 3

0.2-0.4 μmole of the spin label was dispersed in 0.6 ml of distilled water by Vortex agitation, followed by brief sonication, and then 0.3 ml of that dispersion was mixed with 5 mg protein of the membrane pellet (106). The spin labelled membrane suspension contained about 10 mg/ml protein and 0.1-0.2 μmole spin label / ml. EPR spectra were recorded with a Varian EPR spectrometer, model 4502 -15, equipped with a variable temperature controller, model 4540.

Results

Fatty Acyl Composition

Table 1 lists the total fatty acyl composition of the membranes. For arachidic acid supplemented cells, the arachidoyl group comprised about 53% of all acyl groups found in cell membrane lipids. For lauric acid supplemented cells, the sum of myristoyl and palmitoyl groups amounts to 85% of the total fatty acyl groups. For cell grown in an oleic acid supplemented medium, the oleoyl group comprised about 60% of fatty acyl groups found in the cell membrane.

ATPase Activity

ATPase activity of the three types of membranes, enriched as described above, was assayed at different temperatures (Figure 4). At 37^{o}C, the membranes enriched with saturated acyl groups, either short or long ones, have practically the same specific activity. For temperatures below 25^{o}C, the ATPase activity of oleoyl group enriched membranes was higher than that from the other two types of membrane which have virtually the same specific activity. For the ATPase activity of arachidoyl group or short chain enriched membranes, an

Table 1

Fatty acyl composition of total membrane lipid of Acholeplasma laidlawii. Cells were grown in lipid pre-extracted tryptose medium supplemented with fatty acid depleted bovine serum albumin and the fatty acid as indicated.

Fatty acid supplemented	Fatty acyl composition (mole %)									Saturated/unsaturated fatty acyl groups (mole/mole)
	12:0[a]	14:0	14:1	16:0	18:0	18:1[b]	18:2	20:0	UI	
Lauric	3.3	42.0	0.6	42.7	2.4	8.9	-	-	-	9.5
Oleic	1.5	4.6	0.3	26.1	2.2	59.3	-	-	6.1	0.5
Arachidic	1.5	20.2	1.4	16.4	1.6	4.3	1.7	52.8	-	12.5

[a]Number to the left of the colon refers to the number of carbon atoms; the number to the right refers to the number of the double bonds.

[b]Gas chromatographically geometric isomers could not be distinguished. However, infra red spectroscopic analysis of the total fatty acid methyl esters indicated the presence of methyl oleate only.

Figure 4. Arrhenius plot of ATPase activity in membranes isolated from Acholeplasma laidlawii cells grown in a lipid free medium supplemented (6 mg/l) with lauric acid (-■-■-■-), oleic acid (-●-●-●-), or arachidic acid (-▲-▲-▲-). Arrhenius plot (-▲-▲-▲-) of ATPase activity of solubilized (0.1% Triton X-100; 1 mg protein/ml; 1:1, v/v) membranes enriched with arachidoyl groups.

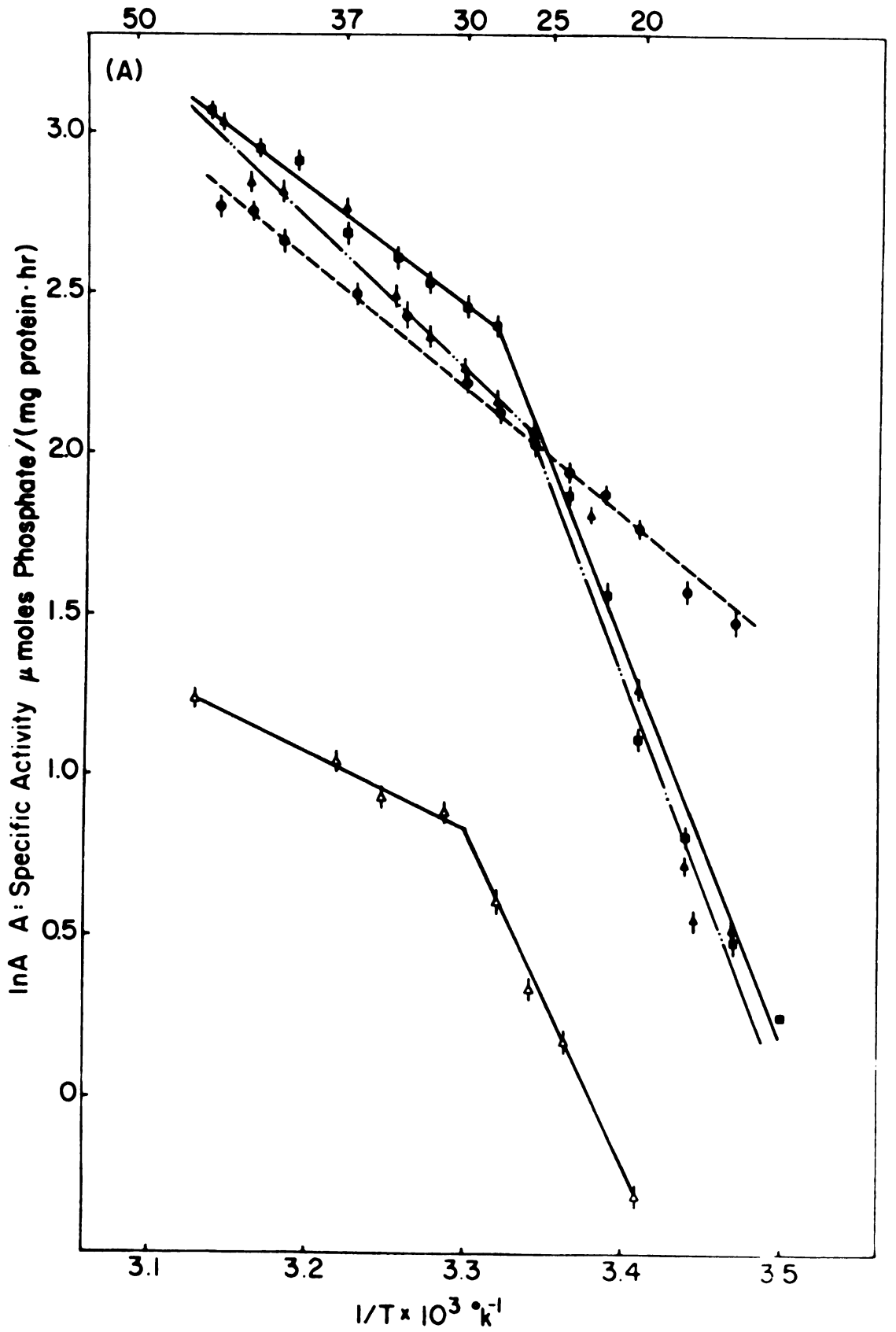
50
37
30
25
20
(A)
3.0
2.5
2.0
1.5
1.0
0.5
0
lnA A: Specific Activity μ moles Phosphate/(mg protein·hr)
3.1
3.2
3.3
3.4
3.5
1/T x 10³ °k⁻¹

Figure 4

Arrhenius plot revealed a biphasic character (Figure 4). The exact temperature where the discontinuity in slope occurred could not be determined; however, it was around 25 - 30°C. For all batches employed, the profile of the Arrhenius plot was always reproducible. The typical plot in Figure 4 shows a slope discontinuity at 26°C for arachidoyl and at 28°C for short chain enriched membranes. From the slope of the Arrhenius plot, the apparent activation energies are about 7-9 kcal/mole and about 25 kcal/mole for saturated acyl group enriched membranes. For oleoyl group enriched membranes, the Arrhenius plot was essentially a straight line; the activation energy was 8±1 kcal/mole.

Membrane Solubilization Studies

Membranes solubilization studies were only carried out with arachidoyl group enriched membranes. The ATPase activity was found in the supernatant. Passing the supernatant through a Sephadex G 200 column, the ATPase activity was associated with the protein which came out from the void volume. This finding is consistent with that described by Ne'eman et al. (113). At any temperature studied, the specific ATPase activity was only 20% that of the non-solubilized material. Apart from the absolute value of the specific enzyme activity, the Arrhenius plots of solubilized and non-solubilized membranes are the same (Figure 4). This may suggest that the solubilized material still contained minute amounts of lipids such that the activation energy remained practically unchanged. This is in agreement with the results reported by Ne'eman et al. (113).

Membrane Fluidity as Measured
By the Spin Labelling Method

Membrane lipid fluidities of the three types of membrane were monitored by the spin labelling method. The fatty acid spin labels were introduced into the isolated membrane in vitro. A representative EPR spectrum is shown in Figure 5. The hyperfine splitting $2T_{\parallel}$ in such a spectrum is related to the molecular order and the rotational mobility of the spin label and therefore reports the local fluidity of the membrane lipids (114,115). A high value of $2T_{\parallel}$ reflects a low local fluidity. Over the entire temperature range (Figure 6), the parameter $2T_{\parallel}$ could be easily determined from spectra taken from 5NS labelled membranes. If membranes were labelled with a 12NS spin label, the high field "dip" in the EPR spectrum became so shallow that an accurate measurement of $2T_{\parallel}$ was impossible. In such a case, the rotational correlation time τ_c of the spin label could be calculated by the following formula (115).

$$\tau_c = 6.5 \times 10^{-10} \times W_0 \times \left(\sqrt{\frac{h_0}{h_{-1}}} - 1 \right) \text{ sec.} \qquad (5)$$

where W_0 is the peak-to-peak width (gauss) of the central resonance peak; h_0 and h_{-1} are the peak heights of the central and high-field peaks respectively.

Around the growth temperature ($37^{o}C$), the three types of membrane tested have approximately the same fluidity (Figure 6). This result is supported by data obtained from 12NS spin labelled membranes. At $37^{o}C$, the correlation time τ_c is 3.16±0.33 nsec for membranes enriched with arachidoyl groups, τ_c = 2.78 ± 0.18 nsec for membranes enriched with short chain saturated acyl chains, and τ_c = 2.80 ± 0.26 nsec for oleoyl

Figure 5. Typical EPR spectrum of the spin label 5NS incorporated *in vitro* into *Acholeplasma laidlawii* membranes enriched with arachidoyl groups. The spectrum was taken from a sample at 25 ^{o}C. The magnetic field strength increases from left to right. $2T_{\parallel}$ is the hyperfine splitting parameter. The vertical arrows indicates signals from unincorporated spin label.

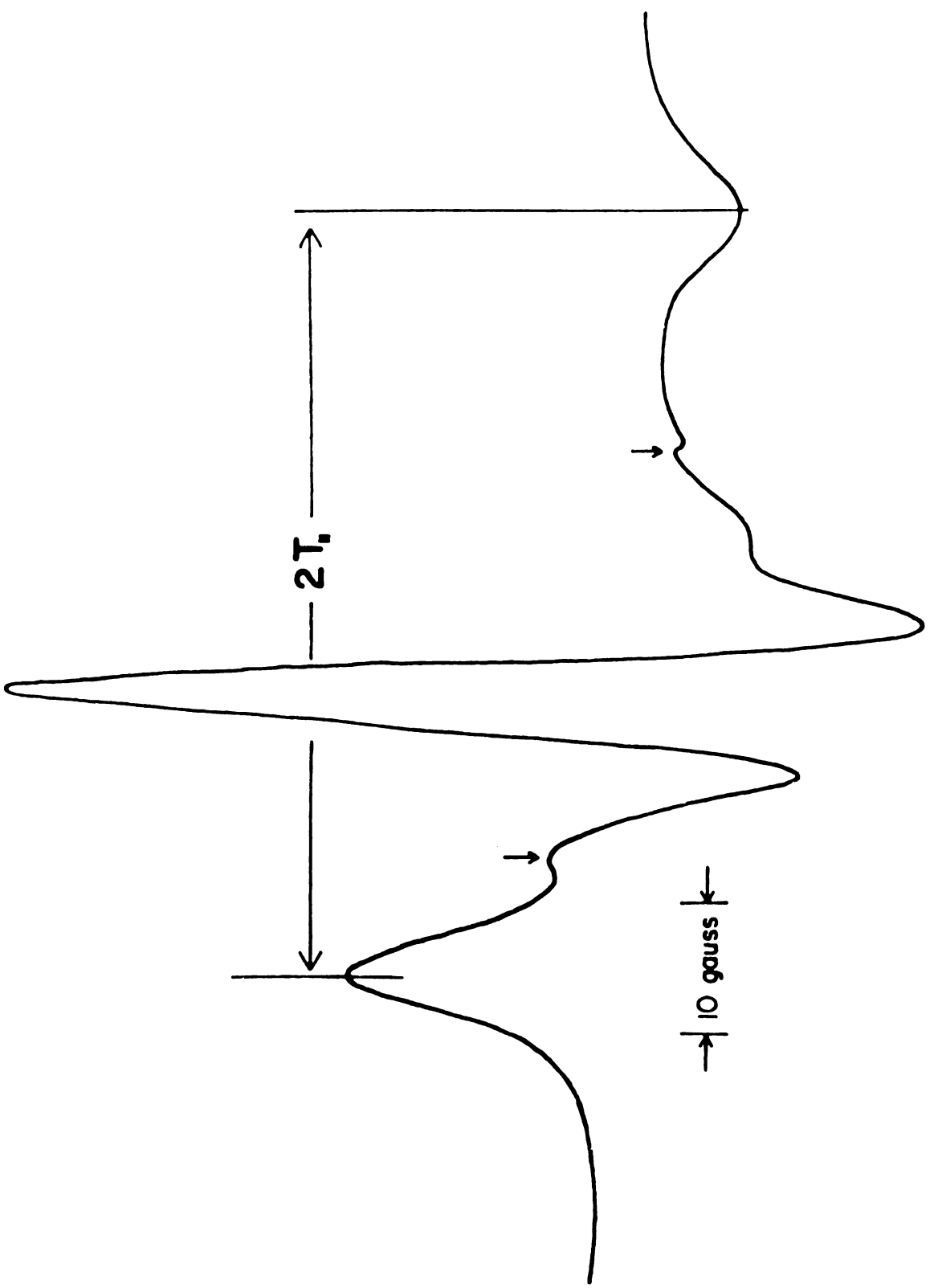

Figure 5

Figure 6. Temperature dependence of the EPR hyperfine splitting parameter $2T_{\parallel}$ as defined in Figure 5. The spin label 5NS was incorporated into membranes isolated from Acholeplasma laidlawii cells grown in a medium supplemented with different fatty acids as explained in Material and Methods. The final concentration of the spin label solution was 0.1-0.2 μm/ml with 10 mg/ml membrane protein.

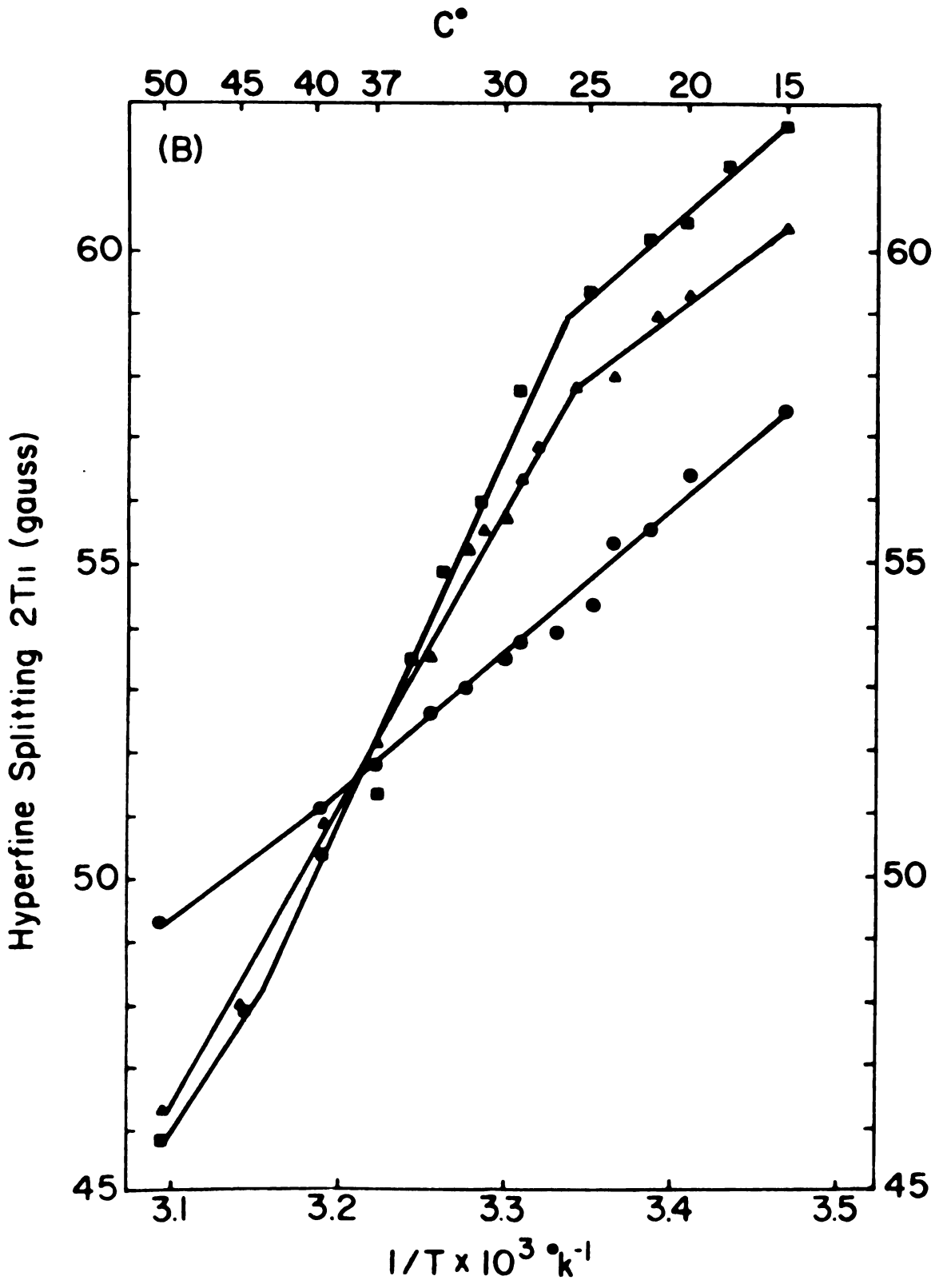
C°
50 45 40 37 30 25 20 15
(B)
60
55
50
45
Hyperfine Splitting 2T|| (gauss)
3.1 3.2 3.3 3.4 3.5
1/T x 10³ °k⁻¹

Figure 6

group enriched membranes, respectively. At temperatures lower than the growth temperature, oleoyl group enriched membranes were appreciably more fluid than the other two types of membrane. For arachidoyl group and short chain ($C_{14:0}$-$C_{16:0}$) enriched membranes, a plot (Figure 6) showed a discontinuity in slope around 26-28^{o}C, whereas in the case of oleoyl group enriched membranes such a discontinuity was absent. The exact point where that discontinuity occurs can not be measured. Such a discontinuity can be interpreted as a liquid/gel like membrane lipid phase transition (116).

Discussion

Our experiments demonstrate that the membrane lipid fluidity and ATPase activity behave similarly with respect to the absence or presence of a discontinuity in slope and also where that discontinuity occured in the Arrihenius plots. A low membrane lipid fluidity is accompanied by a high activation energy for ATPase. This is demonstrated by the following facts: (a) compared to the liquid phase, the activation energy is higher below the discontinuity for ATPase from membranes enriched with saturated acyl chains, and (b) below 25^{o}C both fluidity and enzymatic activity are consistently higher for oleoyl group enriched membranes compared with those enriched with saturated acyl chains.

For the three kinds of membrane studied, the lipid fluidity is practically the same at the growth temperature (37^{o}C), in contrast to the specific enzyme activities which are the same around 25^{o}C. The discrepancy can perhaps be explained by protein aggregation beginning well above the discontinuity in slope (102).

In our experiments we show that the fatty acyl composition does play a role in determining the activation energy for the membrane-bound ATPase. This finding agrees with that reported recently (97), where cholesterol was used to shift the breaking point in the Arrhenius plot. The exogenously administered cholesterol to the non-sterol requiring Acholeplasma represents obviously a nonphysiological perturbation of the membrane. Our system, however, allows one to shift the breaking point (Figure 6) by simply supplying the physiological growth medium with the appropriate fatty acid.

Previously it was reported that Acholeplasma membranes enriched with oleoyl groups have a lower fluidity ($37^{o}C$) as compared to that measured for membranes enriched with saturated acyl chains (100,102). These findings do not agree with ours. The reasons for that discrepancy may be the following ones: Our Acholeplasma laidlawii(oral strain) grows excellently (10^{9} cells/ml within one day) on a nutrient medium supplemented exclusively with arachidic acid (105). Usually cells show a poor growth when cultured in a medium containing long chain fatty acids ($C_{16:0}$,$C_{18:0}$) (28,117). Thus, it is conceivable that those poorly grown cells lack a regulatory mechanism to maintain the membrane lipid fluidity within a narrow range. Upon increase or decrease of the carotenoid content in the Acholeplasma membrane, we have shown that our organism maintains the membrane lipid fluidity within a narrow range by modifying the fatty acyl composition of the lipids (118).

Our results show that all three types of membrane have a practically constant fluidity at the growth temperature, regardless of fatty acid supplementation to the nutrient medium. From a physiological point of view, the cells are able to maintain a constant lipid fluidity within

a narrow range. This capability has been called "homeoviscous adaptation" (119), and was found in Escherichia coli (119) and in Acholeplasma laidlawii (118,120).

The crucial question in interpreting EPR spin labelling data is as to what extent the spin label really reports the microenvironment. Objections regarding the interpretation of spin label results are (a) the perturbation introduced by the spin label and (b) possible non-random distribution of the spin label within the membrane lipids (97). The question of perturbation is as yet not fully answered; there exists evidence for and against this argument (114). Concerning the non-random distribution of the spin label, experiments indicate that fatty acid spin labels prefer the more fluid regions (114,121,122). This criticism may turn out to be advantageous, if the spin label is able to monitor reproducibly those fluid regions where important membrane functions take place. Because of such a preferential localisation, membrane phase transitions are expected to be sharp ones when reported by the spin label, in contrast to broad transitions when monitored by microcalorimetry (97). Microcalorimetry measures the enthalpy which is an average membrane bulk property.

The growth temperature lies generally within the broad lipid phase transition determined by calorimetry (97,121). With the spin labelling method, the relatively sharp transition lies lower than the growth temperature (Figure 6). This latter transition temperature lies approximately around the lower end of the broad lipid phase transition when calorimetric techniques are used (97). This behavior suggests that the spin label provides information about the more fluid membrane lipid regions.

membr

well

a sim

acyl

Our results demonstrate that the breaking points (Figure 4,6) of membrane lipid fluidity and ATPase activity correlate well. This may well indicate that the membrane-bound enzyme and the spin probe are in a similar fluid microenvironment, which depends on the type of fatty acyl chain enrichment of the membrane.

PART TWO

INTRACELLULAR pH AND MEMBRANE POTENTIAL OF *THERMOPLASMA ACIDOPHILA*

CHAPTER III

INTRACELLULAR pH OF THERMOPLASMA ACIDOPHILA

Introduction

Thermoplasma acidophila is a mycoplasma-like organism which grows optimally at 59°C and pH 2 (86). We are interested in the problem of how these cells can live in such a hostile environment without the protection of a cell wall. An electron micrograph from thin sections of Thermoplasma acidophila cells is shown in Figure 7 (123). Since the organism grows under acidic conditions, the question of the intracellular pH becomes significant. If the intracellular pH value should lie in the acidic range, how does the metabolic machinery function? On the other hand, if the intracellular pH lies in the neutral region, how can the cell maintain such a huge hydrogen ion concentration gradient across the membrane?

The intracellular pH was measured by the distribution of a radioactive weak organic acid ^{14}C-labelled 5,5-dimethyl-2,4-oxazolidine-dione (DMO) (Figure 8). This method was first developed for determining the intracellular pH of muscle cells (124), and since then was also applied to the study of pH changes in mitochondria (125), and a few microorganisms (126-128).

Figure 7. An electron micrograph from thin sections of Thermoplasma acidophila cells.
(From reference 123)

Figure 7

Material and Methods

Organism and Growth

Thermoplasma acidophila was grown in a medium containing 1.5 mM $(NH_4)_2SO_4$, 4.2 mM $MgSO_4.7H_2O$, 1.7 mM $CaCl_2.2H_2O$, 0.03% KH_2PO_4 1% glucose, and 0.1% yeast extract (Difco, Detroit, Michigan). The pH was adjust to 2 with concentrated H_2SO_4 and the medium then autoclaved. A 10% (v/v) inoculum from a 22-hr old culture into the same medium gave the best growth. Each culture was continuously aerated for 22 hours with air, sterilized by filtration. Cultures (18 l) were incubated at 56^{o}C in 20 l flasks (129). Cells were harvested at late log phase, after 22 hours of growth, by centrifugation at 15^{o}C, at 9,000 x g for 5 minutes using a Sorval RC 2B centrifuge with a GS 3 rotor. Then, the cells were washed once and resuspended in TG-buffer. The TG-buffer was composed of 0.02N KCl, 0.04 M sucrose, 1.5 mM $(NH_4)_2SO_4$, 4.2 mM $MgSO_4.7\ H_2O$, 1.7 mM $CaCl_2.2\ H_2O$ and 0.01 N glycine buffer at pH_2. This TG-buffer had the same osmolarity, ionic strength and divalent cation concentrations as the growth medium. An 18 l culture usually yielded 35-40 ml of a cellular suspension containing 20-30 mg/ml protein.

Procedure for pH Measurement by the Method of DMO Distribution

In aliquots of 1 ml, that cellular suspension was distributed into a set of centrifugation tubes (size: 4 ml), followed by addition of 1 ml of TG-buffer. A scheme of the procedure is shown in Figure 9. In a typical run, 10 tubes were used to determine gravimetrically the total pellet water, V_t. Another 12 tubes were incubated with 0.1 µCi ^{14}C-dextran (molecular weight 60,000 - 90,000, specific activity 1.31 mCi/mM, New England Nuclear, Boston, Massachusetts) which will not penetrate into

Figure 8. Measurement of intracellular pH by the distribution of a radioactive weak organic acid ^{14}C-labelled 5,5-dimethyl-2,4-oxazolidine-dione (DMO).

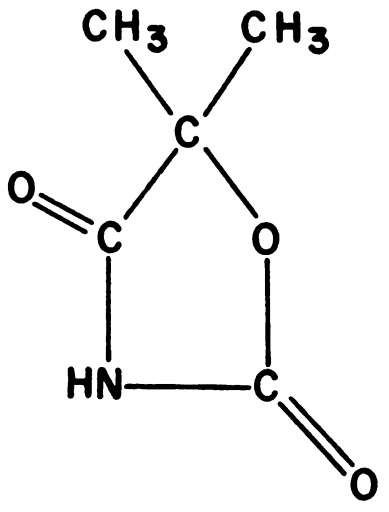

5,5-Dimethyloxazolidine-2,4-dione (DMO-C^{14})

MW = 129.0

pK ~ 6.1 at 56° C

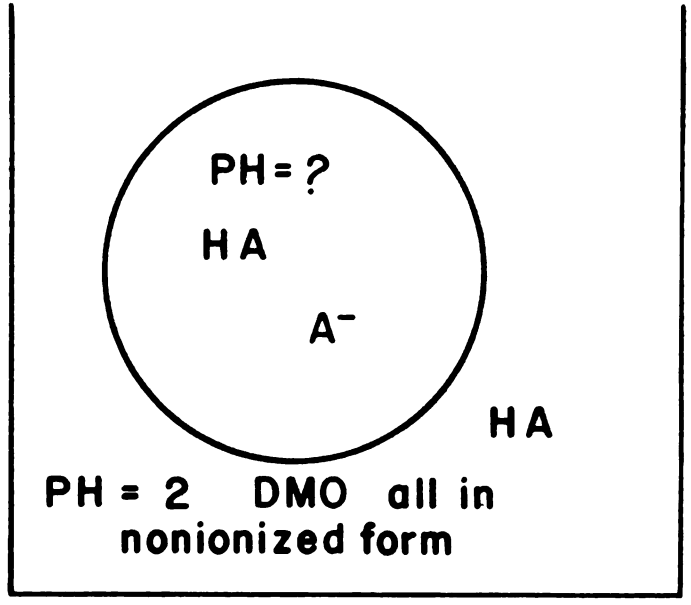

Assumption:

$$(HA)_{out} = (HA)_{in}$$

$$pH_{in} = pK_{in} + \log \frac{(A^-)in}{(HA)in}$$

Figure 8

Figure 9. An experimental scheme of the procedure for measuring intracellular pH by the distribution of DMO.

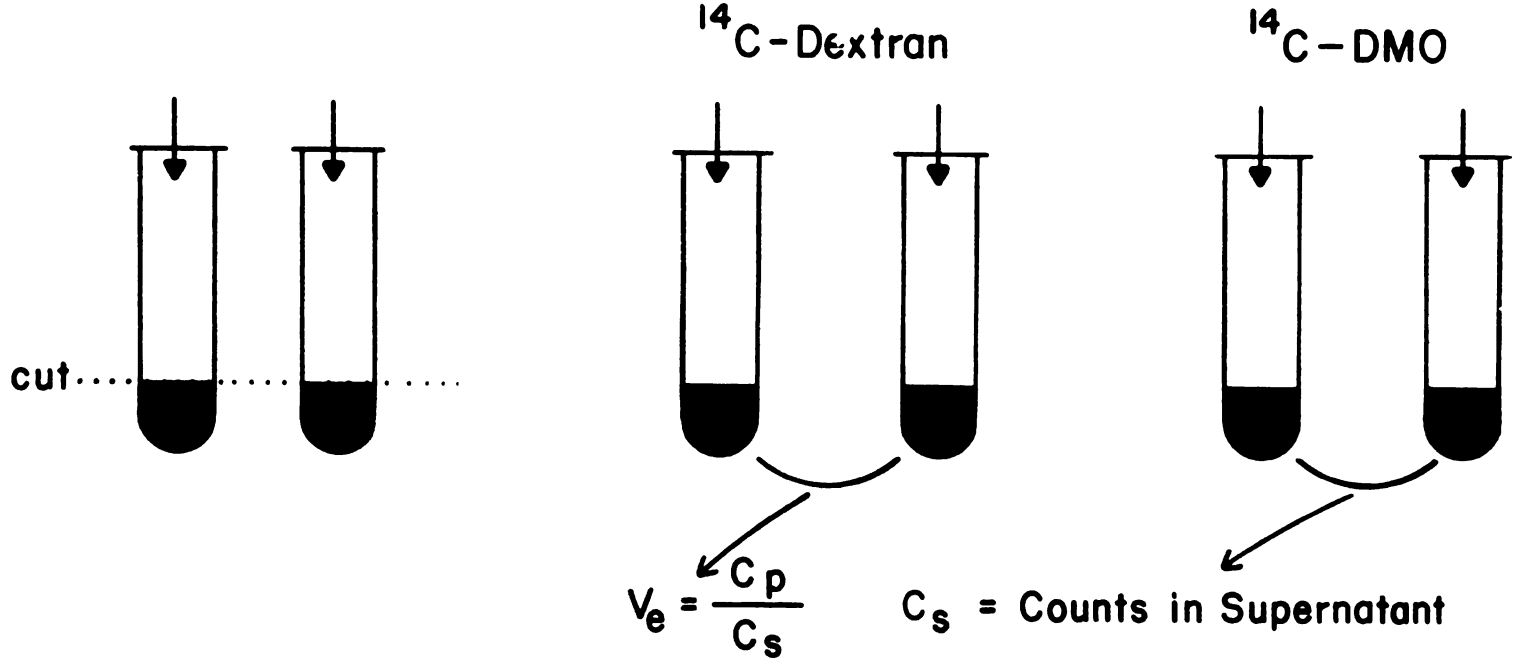

C_s = Counts in Supernatant

C_p = Counts in Pellet

V_p = Total Pellet Water

V_e = Extracellular Pellet Water

Net V_i = Intracellular Water

$$[\text{nonionized form}]_{in} = C_s \cdot V_i$$

$$[\text{ionized form}]_{in} = C_p - C_s V_e - C_s V_i$$

$$pH = pK + \log \frac{[A^-]}{[HA]}$$

Figure 9

the cell, to measure the extracellular pellet water, V_e, An additional 12 tubes were incubated with 0.1 μCi of ^{14}C-labelled DMO (specific activity 11 mCi/mM, New England Nuclear, Boston, Massachusetts) to monitor the intracellular pH. After incubation for one hour at 56^{o}C, or at room temperature, all 34 tubes were chilled to 4^{o}C, then centrifuged simultaneously at 9,000 x g for 10 minutes. Then, the pellets from the ten tubes were cut for gravimetrical determination of total pellet water, weighed immediately, and then dried in an oven for 72 to 96 hours to constant weight. The difference in gram represents V_t in ml. For the rest of the tubes, the supernatant was transferred to test tubes, each pellet was resuspended in 2 ml of TG-buffer in a separate test tube. Then 1 ml from each test tube was dried separately in a scintillation counting vial (Figure 9). After drying, 0.075 ml water and 0.5 ml NCS tissue solubilizer (Amersham/Searle Corp., Arlington Heights, Illinois) was added, followed by addition of 10 ml of a toluene solution containing 3g/l PPO, 0.1g/ldimethyl-POPOP, and counted in a Packard Tricarb scintillation instrument.

Within experimental accuracy the intracellular pH did not depend upon the length of incubation time which was varied from 2 minutes to 2 hours. (Figure 10).

Principle of Using DMO Distribution to Measure Intracellular pH

The principle of employing the distribution of a weak organic acid as a monitor for intracellular pH is based on the assumption that the non-ionized form of the acid permeates passively across the cell membrane and attains equilibrium during incubation, while the ionized form of the weak acid remains practically impermeable to the cellular membrane (124,

Figure 10. The concentration of ^{14}C-DMO inside the cell and in the extracellular pellet space were calculated, and their ratio was related to the incubation time.

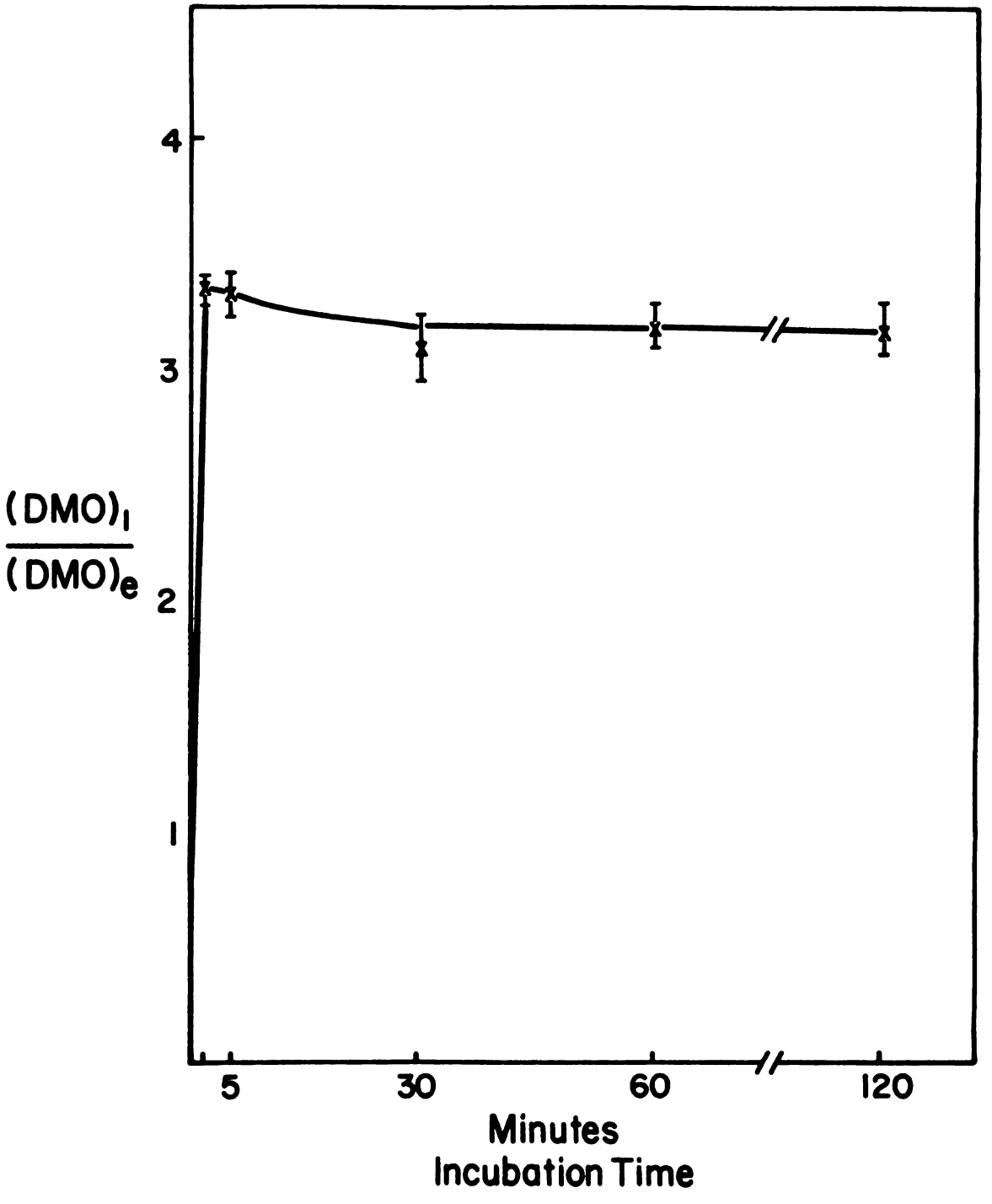

Figure 10

125).

Because DMO has a pK value of 6.1 at 56°C (125), almost all DMO molecules are in the non-ionized form (designated as DMOH) at pH 2 or 4. If the molecule permeates to the interior of the cell, and if the intracellular pH is higher than the pK value, some of the molecules will dissociate from the non-ionized form into the ionized form (designated as DMO^-). The ratio of the two forms at equilibrium can be described by the Henderson-Hasselbach equation (124,125).

$$\text{Intracellular pH} = pK + \log \frac{(DMO^-)}{(DMOH)} \quad \text{.....(6)}$$

Moreover, if DMO passively enters the cell, the intracellular concentration of the non-ionized form will be the same as that of the extracellular non-ionized form. The net result will be an accumulation of DMO in the cell, provided the intracellular pH is higher than the pK value.

But the intracellular concentration of DMO^- and DMOH can not be measured directly. Only the counts of DMO in the supernatant and pellets can be directly measured. If we know the extracellular pellet water and intracellular pellet water we can calculate the intracellular DMO^- and DMOH concentration by the following relationships. These equations hold when extracellular pH<<pK:

Extracellular water $V_e = C_p$ (dextran)/C_s (dextran).....(7)

Here, C_p (dextran) are the counts of (^{14}C) dextran per pellet.

C_s (dextran) are the counts of (^{14}C) dextran per ml of supernatant.

Intracellular water volume $V_i = V_t - V_e$.....(8)

Intracellular concentration of ionized form

$$C_i(DMO^-) = \{C_p\ (DMO) - C_s(DMO) \times V_t\}/\ V_i \quad \text{.....(9)}$$

Intracellular concentration of non-ionized form C_n (DMOH)

$$C_n\ (DMOH) = C_s\ (DMO) \quad \ldots\ldots\ldots\ldots\ldots\ldots\ldots\ldots\ldots\ldots (10)$$

From equation 9, equation 10, and equation 6, we get:

$$\text{Intracellular pH} = pK + \log\ (C_i\ /C_n) \quad \ldots\ldots\ldots\ldots\ldots (11)$$

When the extracellular pH is close to the pK of DMO, the equations can be easily modified by calculating the percentage of DMO in the non-ionized form at this particular external pH. For example, when the external pH is at 6, approximately half of the DMO is in non-ionized form.

Direct pH Measurement

After being harvested, Thermoplasma acidophila cells were washed ten times with distilled water, and 1 gram of pellet was sonicated one hour with a Raytheon Sonic Oscillator, model DF-101, operated at 0.92 A.

Direct pH measurements of the sonicated material were performed with a Beckman micro blood assembly, No. 46 850, attached to an Orion digital pH meter, model 801.

Malate Dehydrogenase Assay

The malate dehydrogenase activity was measured in the forward direction (oxaloacetate + NADH→ malate + NAD), the standard reaction mixture contained 125 μM oxaloacetate, 50 μM NADH, 25 mM of either glycine, glycyl-glycine, phosphate, or acetate buffer, and 10-50 μl membrane preparation in a total volume of 3.0 ml. The reaction mixture was incubated at 56°C and the absorbance decrease of NADH was monitored at 340 nm with a Gilford spectrophotometer, model 2400, equipped with a digital absorbance meter and automatic recorder (130).

Results and Discussions

Intracellular pH Measured by the Distribution of DMO

The intracellular pH lies in the range from 6.4 to 6.9 (Table 2). The average variation within the same set of experiments is about 0.05 pH units. However, the variation between different sets of experiments amounts to 0.5 pH unit maximally. This may result from biological variation or from errors in the estimation of the intracellular water volume, V_i. But the error caused by this is very small, for example, a 100% error of V_i would change the pH value only by 0.3 units. Therefore we conclude that the intracellular pH of Thermoplasma acidophila is close to neutral.

Validity of Using DMO Distribution as a Method to Measure Intracellular pH

To test whether DMO molecules are passively transported across the cell membrane, dilution experiments were undertaken to determine whether the radioactive DMO accumulated inside the cells could be readily washed out. If the cells were initially loaded with radioactive DMO (60 000 cpm in the supernatant, and 24 000 cpm in the pellet of 20 mg protein, after centrifugation), then washed with TG-buffer, the counts in the supernatant C_s(DMO) and in the pellet C_p(DMO) decreased linearly and parallel to each other, and when plotted on a semi-logarithmic paper, within three washes by three orders of magnitude (Figure 11). Additional experiments were carried out to determine the ratio of intracellular DMO concentration to extracellular DMO concentration. Using six different DMO concentrations (1.7×10^4-3.1×10^5 cpm/ml), the ratio remained at a constant value of about 2.5 (Figure 12). The ratio will also not change

Table 2

Determination of the intracellular pH in Thermoplasma acidophila cells by measuring the distribution of radioactive 5,5-dimethyl-2,4-oxazolidinedione across the plasma membrane[a].

	Exp.[b] 1	Exp.[b] 2	Control[b]	Cells Boiled for 5 hrs.[c]
C_s(dextran-^{14}C), cpmx10^3	57.7±1.2	124.6±3.7	90.7±6.1	82.6±1.6
C_p(dextran-^{14}C), cpmx10^3	2.70±0.06	7.74±0.40	4.67±0.19	3.79±0.19
V_t, µl	132±3	133±4	122±1	103±0.5
V_e, µl	103±4	117±5	103±4	90.6±2
V_i, µl	29±7	16±9	19±5	12.4±2.5
C_s(DMO-^{14}C), cpmx10^3	33.3±0.7	209.6±5.3	50.8±1.3	45.9±7.6
C_p(DMO-^{14}C), cpmx10^3	4.48±0.01	18.6±0.41	36.6±0.75	27.41±0.67
Ionized form, pmx10^3	4.47±0.01	9.27±0.23	19.9±1.8	12.44±0.57
Nonionized form, cpmx10^3	0.94±0.05	3.21±0.11	9.42±0.24	5.67±0.09
Intracellular pH	6.84±0.04	6.56±0.02	6.41±0.06	6.46±0.05

[a] C_s are the counts of 1 ml supernatant; C_p are the counts of 1 ml of resuspended pellet material. V_t is the total pellet water measured gravimetrically; V_e is the extracellular pellet water; $V_i = V_t - V_e$ is the dextran-impermeable space. The intracellular pH was calculated from the ratio of the concentration of the intracellular ionized form to that of the non-ionized form of DMO (Eqn. 2-3).

Table 2 (cont'd.)

	Control[b]	Cells with 2,4 DNP 0.1 mM[c]	Control[b]	Cells with Iodoacetate 10 mM[c]	Control[b]	Cells with NaN_3 10 mM[c]
C_s(dextran-^{14}C) cpmx10^3	58.1±.6	57.3±.8	66.1±1.6	66.4±1.6	50.1±.9	48.4±1.8
C_p(dextran-^{14}C) cpmx10^3	2.66±.08	2.65±.05	4.06±.19	4.08±.20	3.51±.16	3.46±.17
V_t, µl	118±1	118±1	137.3±1.6	137±3	156±4	156±4
V_e, µl	91.5±3	92.4±2	124±56	123±6	140±7	142±6
V_i, µl	26.5±4	25.6±3	13.3±57.6	14±9	16±11	14±10
C_s(DMO-^{14}C) cpmx10^3	139.0±8.1	147.8±4	82.4±3.5	82.4±3.3	97.1±3.5	87.5±5.5
C_p(DMO-^{14}C) cpmx10^3	13.31±.13	13.0±.09	6.57±.06	6.40±.18	9.24±.15	8.69±.29
Ionized form cpmx10^3	12.9±.87	11.1±.57	3.18±.13	2.77±.14	4.68±.14	5.47±.30
Nonionized form cpmx10^3	3.58±.21	3.73±.10	1.12±.05	1.19±.05	1.41±.09	1.31±.07
Intracellular pH	6.66±.06	6.57±.04	6.56±.06	6.47±.09	6.62±.07	6.72±.06

[b] Typical experiments and controls showing the range and variability of the intracellular pH from different batches of cells.

[c] Influence of heat and inhibitor treatments upon intracellular pH, measured parallel to a control from the same cell batch.

Figure 11. The effect of washing on the accumulation of radioactive DMO. Both supernatant and pellet counts show linear decrease in a semi-logarithmic plot.

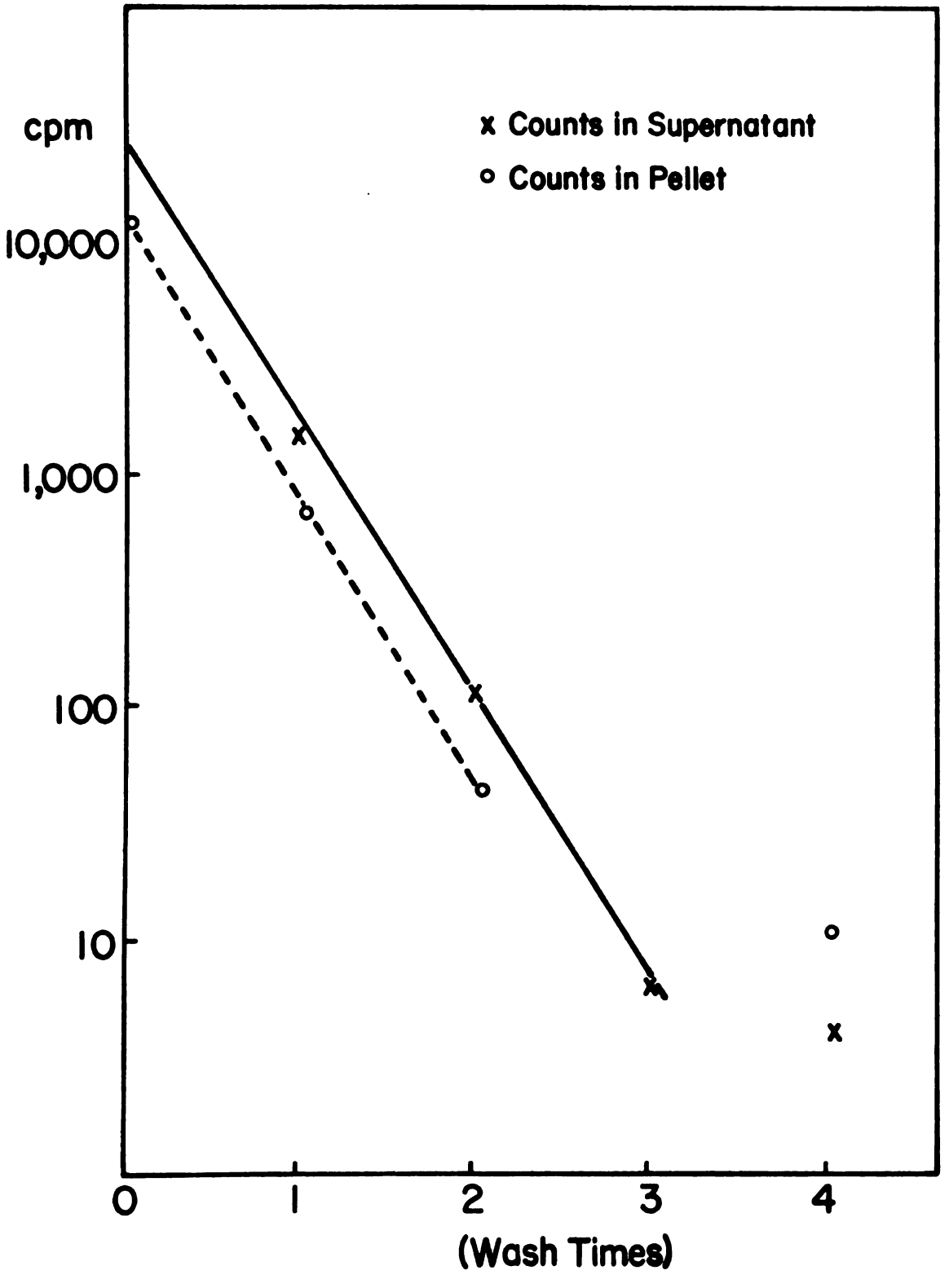
cpm
x Counts in Supernatant
o Counts in Pellet
10,000
1,000
100
10
0
1
2
3
4
(Wash Times)

Figure 11

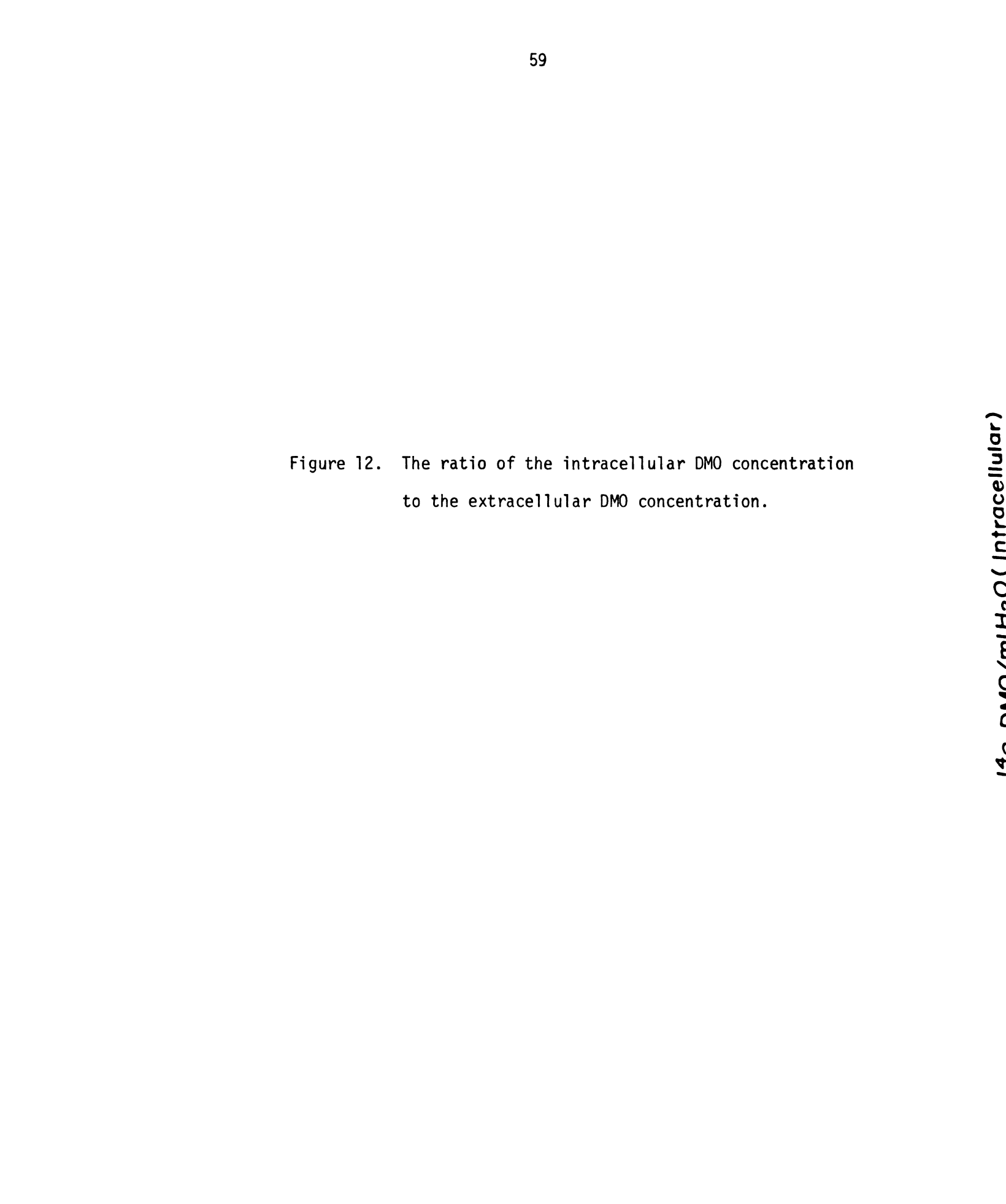

Figure 12. The ratio of the intracellular DMO concentration to the extracellular DMO concentration.

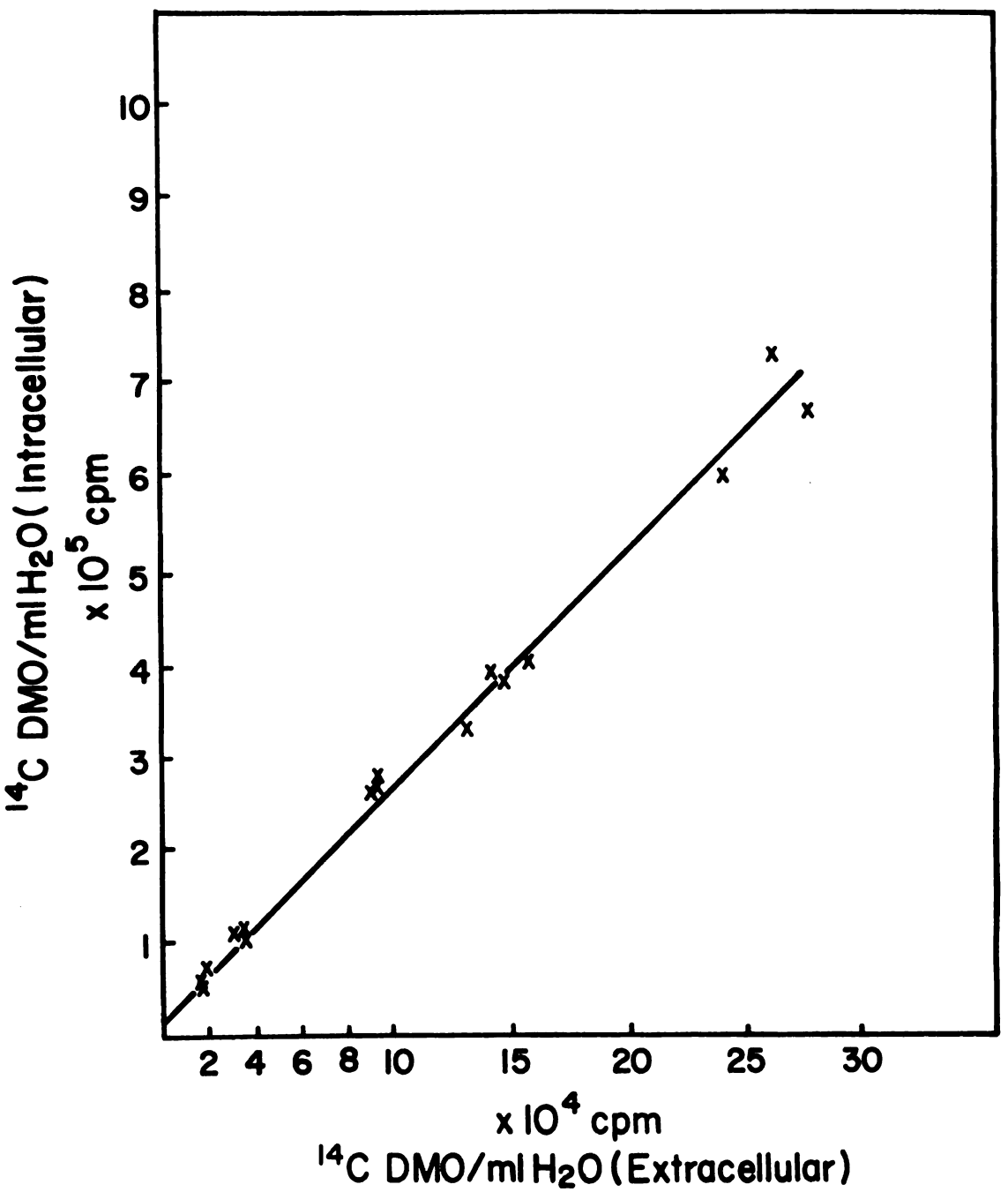
10
9
8
7
6
5
4
3
2
1
^{14}C DMO/ml H_2O (Intracellular)
x 10^5 cpm
2 4 6 8 10 15 20 25 30
x 10^4 cpm
^{14}C DMO/ml H_2O (Extracellular)

Figure 12

when the external DMO concentration was increased with nonradioactive DMO up to 10 mM/l. These results support the assumption that DMO is passively transported into the cell, i.e., no substrate specific, saturable, energy dependent accumulation of DMO into the cell. Physiologically, DMO (molecular structure as shown in Figure 8), which is not an analogue to any known metabolite, is a rather foreign molecule to the cell; and therefore, it is difficult to imagine that the cell can actively transport this "non-natural" molecule.

As to the validity of the second requirement of the DMO distribution method, there exists no direct way to verify whether the ionized form is actually impermeant to the cell membrane. Comparing the rate of lysing of Streptococus faecalis protoplasts at pH 5.3 and 7.5, it was found that the ionized form of DMO penetrates at least 200 times more slowly than the non-ionized form (126). However, the difference of the concentration of the non-ionized DMO form at pH 5.3 and 7.5 amounts to $10^{2.2}$ = 158 fold. The rate of passive penetration of non-ionized DMO is proportional to the concentration. Thus, the ratio of the permeability coefficient of the non-ionized form to that of the ionized form of DMO should be significantly slower than 200 fold. This argument is consistent with our experimental finding that the ratio $(DMO)_i/(DMO)_o$, and consequently the intracellular pH value, do not depend upon the length of incubation time (2 minutes - 2 hours) (Figure 10). Furthermore, the fact that DMO can be accumulated in the cell speaks against the assumption that DMO^- is permeable to the cell membrane; if that were the case, we would not see the accumulation of DMO and would rather obtain an apparent intracellular pH value in the very acidic range.

Other Evidence Concerning the Intracellular pH

There are three independent lines of evidence suggesting that the intracellular pH lies in the neutral region. Firstly, after being harvested, Thermoplasma acidophila cells were washed ten times with distilled water, then the pellet was sonicated for one hour, transmission electron micrographs showed broken cells (129). Then, the pH of sonication fluid was measured directly with a Beckman micro blood assembly, and was found varying from 6.1 to 6.8. Without extensive washing, a lower value near pH 5.5 may be the result of direct measurement, presumably from the contamination of trace amounts of the medium at pH 2 at the external surface of the cell. Secondly, cells (10 mg/ml protein) titrated with 0.04N NaOH have shown a titration curve with an inflection point around 6.5 to 6.9 (Figure 13). At pH 9.3 the cells lyse, the cytoplasm could be collected, and it started to precipitate when the pH became close to neutral (129). Thirdly, we also demonstrated that Thermoplasma acidophila has malate dehydrogenase activity associated with the cytoplasm fraction. This enzyme is easy to assay and known to exist in various higher organisms (130-133). The enzymatic activity was assayed in four different buffers ranging from pH 3 to 12 (134). A pH profile of that enzyme has a broad optimum from pH 8.5 to 10 (Figure 14), and the activity is less than 25% for pH values lower than 6.5. Such a profile is typical for that enzyme in higher organisms (130-133). Similarly the pH profile of Mg-ATPase activity measured by Yang, L. in this laboratory (personal communication) also showed optimum activity above pH 7, with little activity at a pH below 6.5. These facts also indicate that the intracellular pH is near neutral.

Figure 13. Effect of pH on cell lysis.

•—• pH change in an aqueous cell suspension (6 mg.ml) upon dropwise addition of 0.04N NaOH.

X— X Release of protein observed when an aqueous suspension of cells (6 mg/ml) is diluted ten-fold by buffers of varying pH. All buffers used were 1M. Buffer at pH 9, 10 and 11 were glycine-NaOH; at pH 8 and 4, citrate-NaOH; at pH 5,6, 7 phosphate-NaOH.

(From reference 129)

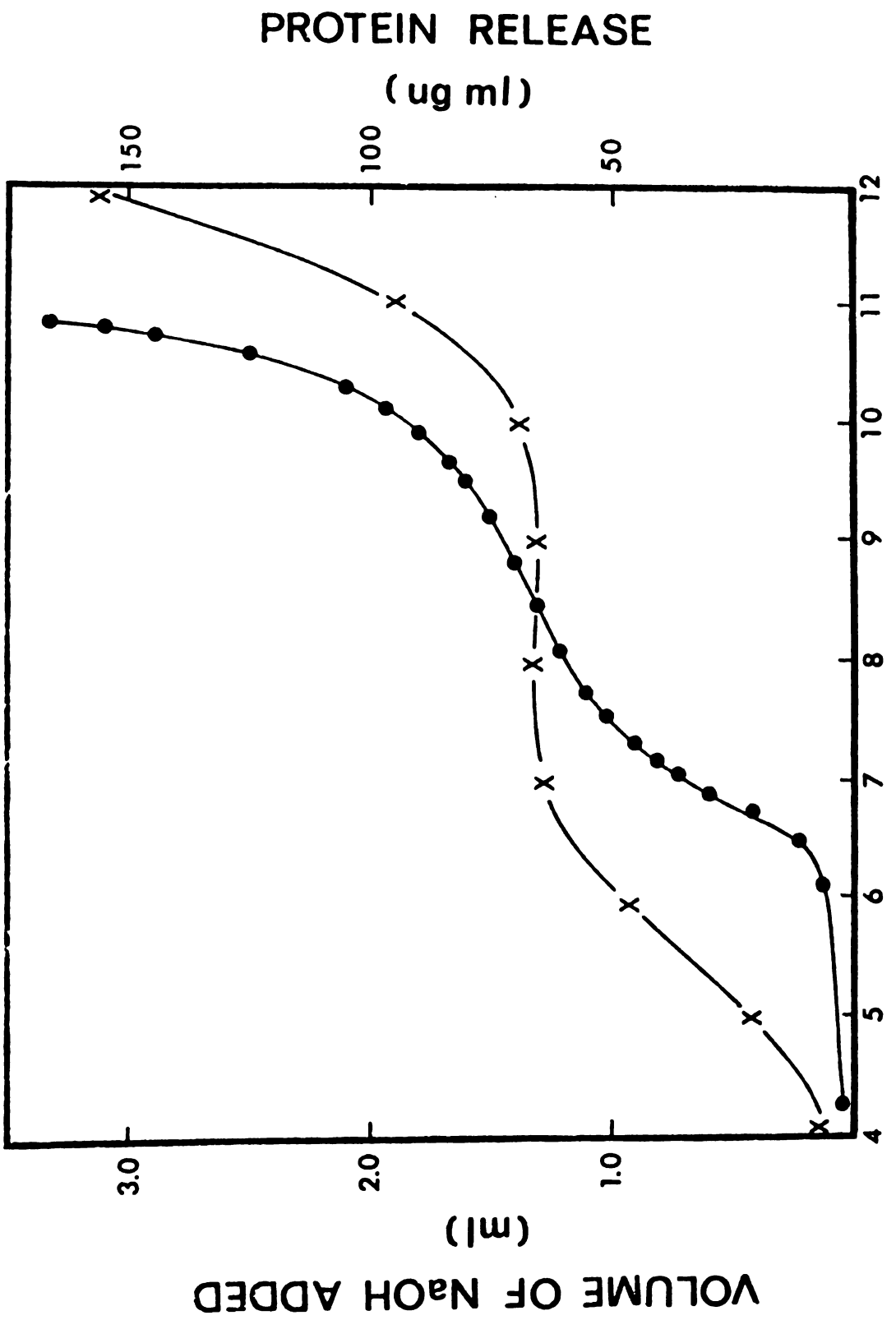
PROTEIN RELEASE
(ug ml)
150
100
50
VOLUME OF NaOH ADDED
(ml)
3.0
2.0
1.0
pH
4
5
6
7
8
9
10
11
12

Figure 13

Figure 14. The pH profile of cytoplasmic malate dehydrogenase from Thermoplasma acidophila, assayed in four different buffers at 56 ^{o}C. The enzymatic activity was measured by reduction of oxaloacetate and monitoring the absorbance decrease of NADH at 340 nm.

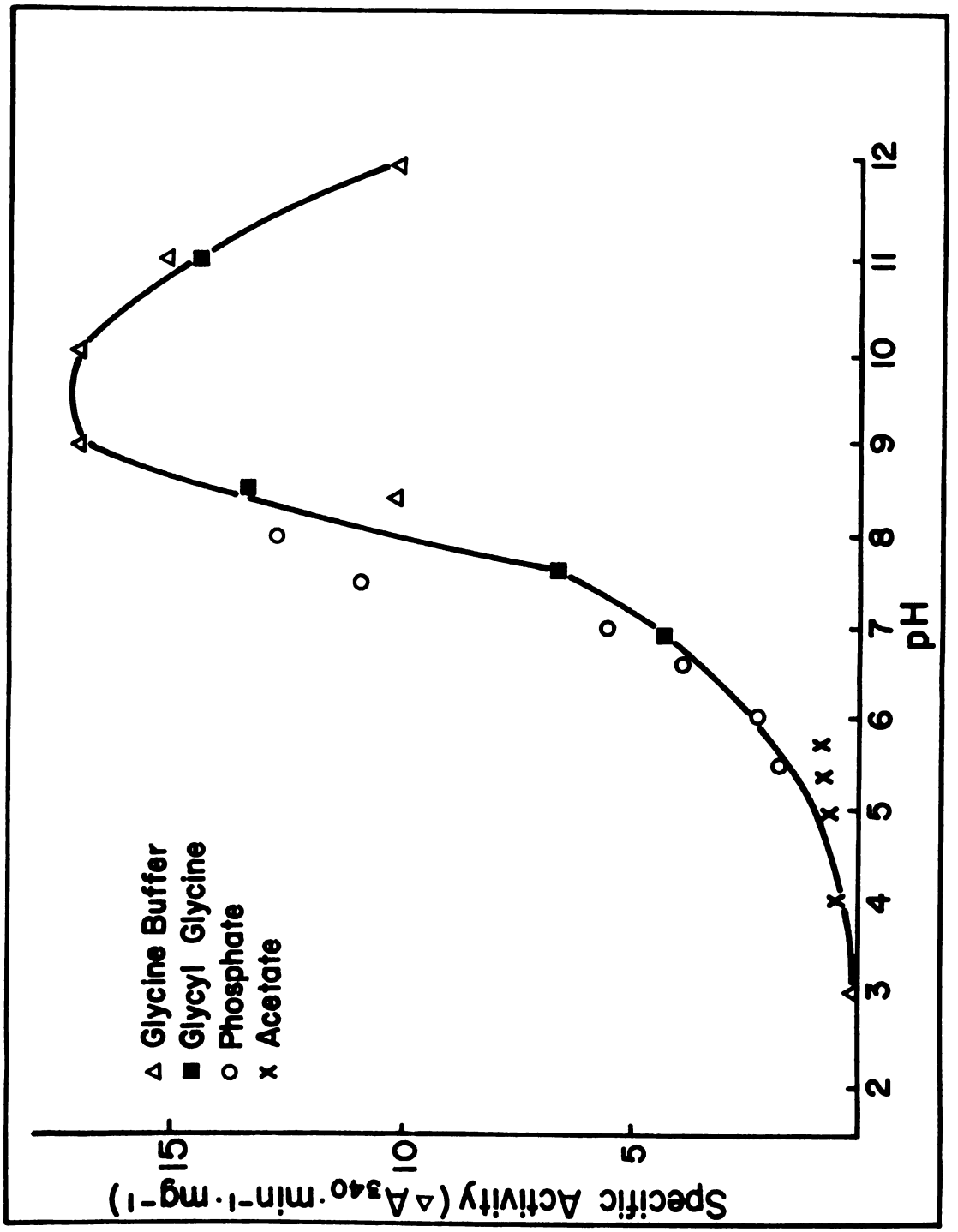
Specific Activity ($\Delta A_{340} \cdot min^{-1} \cdot mg^{-1}$)
15
10
5
2
3
4
5
6
7
8
9
10
11
12
pH
Glycine Buffer
Glycyl Glycine
Phosphate
Acetate

Figure 14

Influence of Temperature and External pH on Intracellular pH

Within experimental accuracy, the intracellular pH as measured by the DMO distribution method is not affected by temperature changes (56^{o}, 24^{o}), or by alteration of the extracellular pH from 2 to 6 (Figure 15). At pH 4 and 6, the cells were suspended in TC-buffer, which is TG-buffer, where citrate replaced the glycine. Moreover, to calculate the intracellular pH of cells in TC-buffer at pH 6, we assumed that in the extracellular medium, half of the number of DMO molecules are in ionized form, and the other half are in the non-ionized form. Thus, the cells are capable to maintain the intracellular pH when subjected to those environmental alterations.

How Is the Hydrogen Ion Concentration Gradient Maintained?

We explored whether Thermoplasma acidophila cells require active metabolic processes to maintain the hydrogen ion concentration gradient of 4.5 pH units, or whether passive mechanisms play an important role. When Thermoplasma acidophila cells were boiled for five hours at 100^{o}, the intracellular pH measured at the end of the harsh treatment was still neutral (Table 2). These boiled cells were no longer viable as demonstrated by inoculating them into culture medium.

By exposing viable cells to general metabolic inhibitors, such as 0.1 mM 2,4-dinitrophenol, 10 mM iodoacetate and 10 mM sodium azide, growth of cultured cells was prevented. None of these inhibitors altered the intracellular pH within experimental accuracy (Table 2). On the basis of these heat and inhibitor treatments, we therefore conclude that the major portion of the pH gradient is not maintained by active

Figure 15. The effect of external pH on the intracellular pH of Thermoplasma acidophila. For pH 2, the suspension medium was composed of 0.02N KCl, 0.04M sucrose, 1.5mM $(NH_4)_2SO_4$, 4.2mM $MgSO_4.7H_2O$, 1.7mM $CaCl_2.2H_2O$ and 0.01N glycine buffer. For pH 4 and 6, the glycine buffer was replaced by citrate buffer.

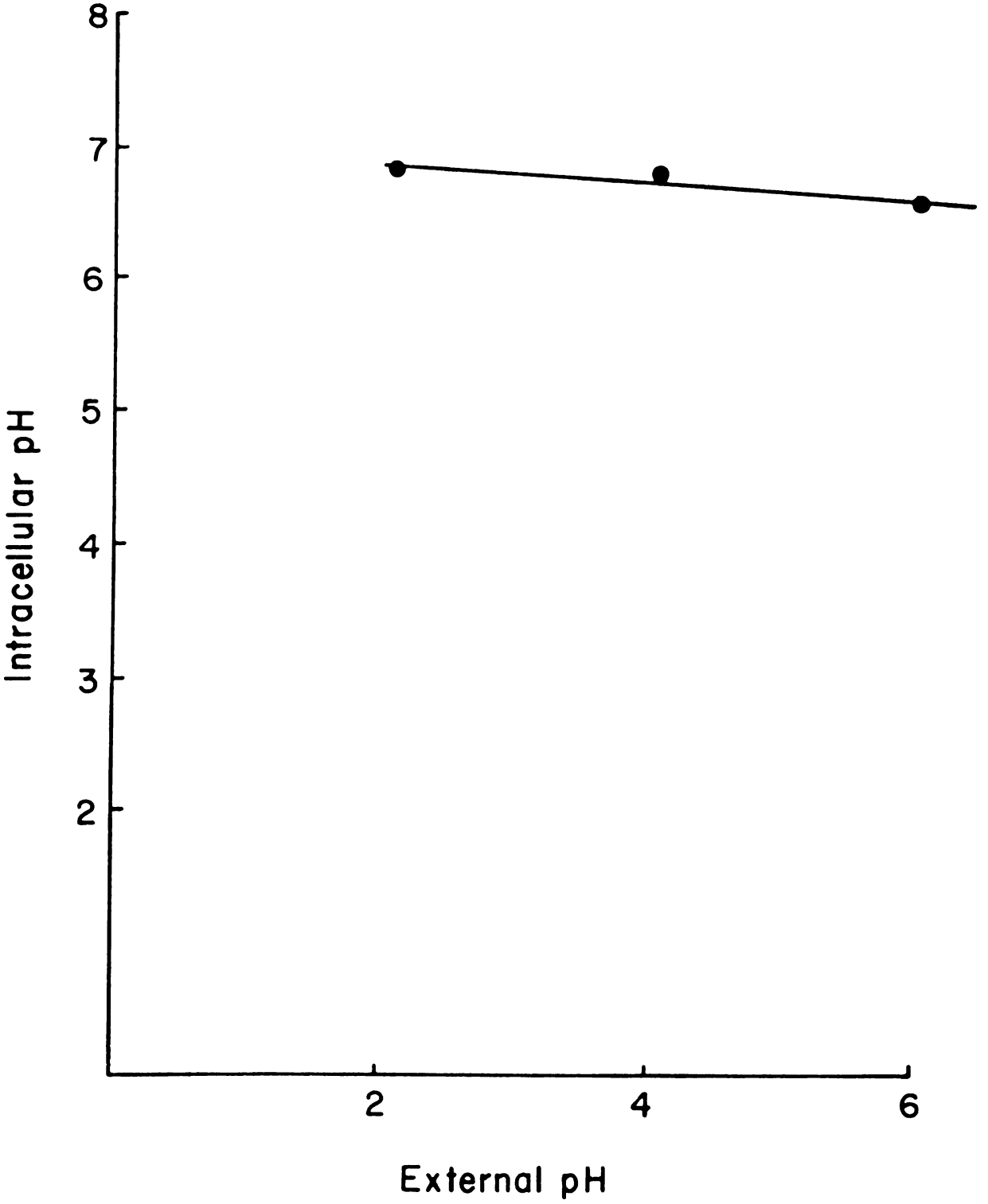

Figure 15

processes, but rather by passive properties of the cell. A Donnan potential across the membrane generated by charged macromolecules impermeant to the cell membrane, can account for maintenance of the huge hydrogen ion concentration gradient without participation of active mechanisms.

CHAPTER IV

MEMBRANE POTENTIAL AND SURFACE CHARGE OF *THERMOPLASMA ACIDOPHILA*

Introduction

Thermoplasma acidophila is a mycoplasma-like organism which grows optimally at 59°C and pH 2, and stops growing above pH 4 (86). The intracellular pH lies between 6.4 and 6.9 as determined by the distribution of a radioactive weak organic acid, 5,5-dimethyl-2,4-oxazolidine-dione (DMO). The cell can maintain this pH gradient of about 4.5 pH units when subjected to metabolic inhibitors, such as iodoacetate, NaN_3, and 2,4-dinitrophenol (134). Because the cell can passively maintain such a huge pH gradient across the membrane, we propose that a Donnan potential exists, possibly generated by charged macromolecules impermeable to the cell membranes. To test this hypothesis, the membrane potential was measured by the distribution of radioactive $KS^{14}CN$, which is known to permeate biological membrane (135,136). Furthermore, a radioactive lipophilic cation tetraethyl-ammonium (TEA^+) was used to determine the polarity of the cell.

The surface charge density and the ζ potential, i.e., the potential difference from the cell surface of shear relative to the bulk medium can be estimated from the electrophoretic mobility of the cell. The

movement of the cell in an applied electric field can be observed directly under a microscope (137-139).

The Helmholtz-Smoluchowski equation

$$u = \frac{D\,\zeta}{4\pi\eta} \tag{12}$$

and

$$\sigma = \sqrt{\frac{NDkT}{2000}} \times \sqrt{\sum c_i [\exp(-z_i e/kT) - 1]} \tag{13}$$

can be used for the calculation of the zeta-potential and the surface charge density (138-142). Here, u = electrophoretic mobility (velocity/unit field strength), ζ = potential difference between the surface of shear and the bulk of the liquid, D = dielectric constant, η = viscosity of the suspension medium, σ = surface charge density. c_i are molar concentrations of ions with charge z_i, N = Avogadro number, k = Boltzmann constant, e = electron charge.

These equations are valid for large smooth particles at an ionic strength such that $\kappa\alpha > 100$. Here, α is the radius of curvature of the cell surface. κ is the Debye-Hückel constant defined as

$$\kappa = \sqrt{\frac{8\,N\,e^2}{1000\,DkT}} \cdot \sqrt{\frac{1}{2}\sum c_i \cdot z_i} \tag{14}$$

For Thermoplasma acidophila with a diameter of 0.5 to 1 μm, this condition generally holds for the ionic strengths used in this investigation. From the potential difference between the bulk phase of the external medium and that of the cytoplasm, and the zeta-potential, the potential profile between the two interfaces of the plasma membrane can be constructed.

Material and Methods

Growth of Cells and Harvest

Thermoplasma acidophila was grown as described previously (134). Aerated 18 l cultures were harvested at late log phase, after 22 hours of growth, by centrifugation at 9,000 x g, at 15°C for 5 minutes. Then the cells were washed twice and resuspended in 1.5 mM $(NH_4)_2SO_4$, 4.2 mM $MgSO_4.7H_2O$, 1.7 mM $CaCl_2$. 2 H_2O, 0.04 M sucrose and 0.01 M glycine buffer, pH 2. This medium has the same ionic strength, osmolarity, and divalent cation concentration as the growth medium. An 18 l culture usually yielded 35 to 40 ml of a cellular suspension containing 20 to 30 mg/ml protein. In aliquots of 1 ml, that cellular suspension was distributed into a set of centrifugation tubes (size 4 ml), followed by addition of 1 ml of the suspension buffer mentioned above to each tube.

Procedure of Measuring Membrane Potential by the Distribution of SCN^-

In a typical experiment (Figure 16), 8 tubes were used for gravimetrically determining the total pellet water, V_t, 8 tubes were incubated with ^{14}C-dextran (molecular weight 60,000 - 90,000), 0.1 μCi, specific activity 1.31 mCi/mM (New England Nuclear, Boston, Massachusetts), to measure the extracellular pellet water, V_e. In addition, 8 tubes were incubated with 0.1 μCi $KS^{14}CN$ (60 mCi/mM specific activity, Amersham/Searle, Arlington Heights, Illinois), and 8 tubes with 0.1 μCi ^{14}C-labelled tetraethylammonium bromide (TEAB) (2.8 mCi/mM, New England Nuclear, Boston, Massachusetts). After incubation for one hour at 56 °C (the amount of KSCN accumulated in the cells did not depend upon the length of incubation which was varied from 10 minutes to 2 hours), all

Figure 16. An experimental scheme of the principle and precedure for measuring the membrane potential by the distribution of SCN^-.

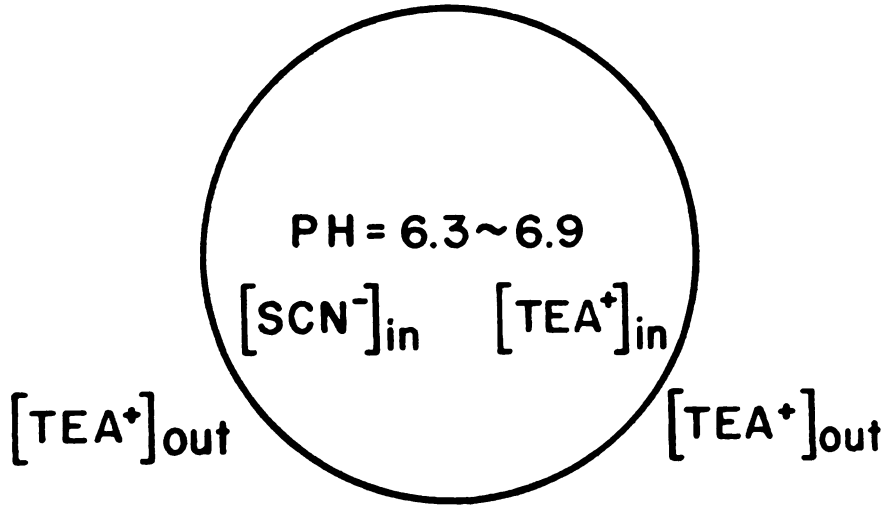

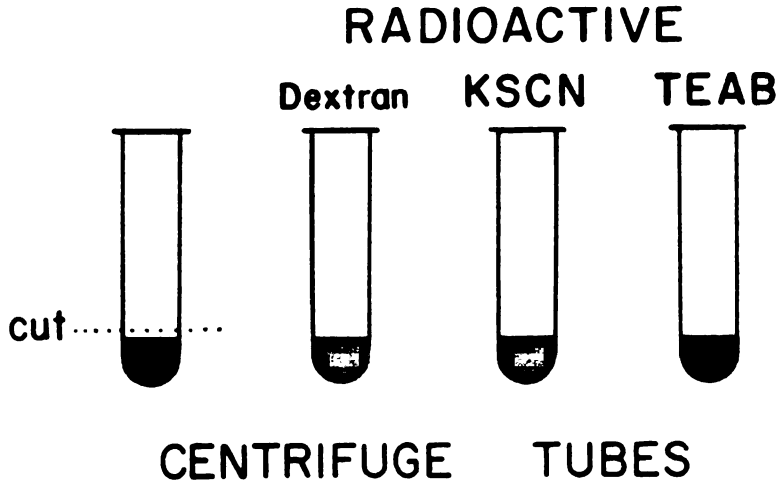

$$\Psi = \frac{RT}{NF} \ln \frac{[SCN]_{in}}{[SCN]_{out}}$$

$$V_e = \frac{Cs/ml}{Cp}$$

$$V_i = V_t - V_e$$

$$[SCN^-]_{out} = Cs/ml$$

$$[SCN^-]_{in} = (Cp - Cs \cdot Ve) / Vi$$

Figure 16

32 tubes were chilled to 4°C, then centrifuged simultaneously at 9,000 xg, at 4°C, for 10 minutes. The supernatant was transferred to test tubes, each pellet was resuspended in 2 ml of the above mentioned suspension buffer in a separate test tube. 1 ml from each test tube was dried separately in a scintillation counting vial. After drying, 0.065 ml water and 0.5 ml NCS tissue solubilizer (Amersham/Searle Corp. Arlington Heights, Illinois) was added, followed by addition of 10 ml of a toluene solution containing PPO (3g/l) and dimethyl-POPOP (0.1g/l), and counted in a Packard Tricarb scintillation instrument.

The intracellular water volume is $V_i = V_t - V_e$.....(15)

Where $V_e = C_p$ (dextran)/C_s (dextran).....(16)

Here C_p are the counts of total pellet material

and C_s are the counts per milliliter of supernatant.

The intracellular concentration of SCN^- is calculated from:

$$[SCN^-]_{in} = [C_p(SCN^-) - C_s(SCN^-) \cdot V_e]/V_i \qquad (17)$$

The membrane potential Ψ, positive inside, was calculated from:

$$\Psi = \frac{RT}{F} \ln \frac{[SCN^-]_{in}}{[SCN^-]_{out}} = 65 \log \frac{[SCN^-]_{in}}{[SCN^-]_{out}} \quad \text{at } 56^oC. \qquad (18)$$

Microscopic Electrophoresis

The electrophoresis instrument used was a Northrop-Kunitz cataphoresis unit, purchased from Thomas Scientific Co., Philadelphia, Pa. The electrophoretic cell was mounted on the stage of a Zeiss Photomicroscope which was equipped with a planachromatic objective 16 x / 0.35. The depth of the cataphoresis chamber was 380μm as

determined with a micrometer scale on the fine adjustment of the microscope. A Sony video camera was attached to the microscope and connected to a Sony-matic video recorder, model AV-3600, and also to a Sony Electrohome TV monitor. A Heathkit regulated power supply, Model IP-17, was used as a constant voltage source. The distance between the two tips of the platinum electrodes in the centre chamber was 3.2 cm. The potential difference between these tips was monitored at the beginning, end, and occasionally during the experiments with a potential meter; it measured 36V, when 200 V were applied, and 17.5 V, when 100 V were applied at the Zn-$ZnSO_4$ electrodes (1N $ZnSO_4$).

The movement of the Thermoplasma acidophila cells was visually observed and recorded on video tapes. The distance travelled was observed and recorded on video tapes. The distance travelled was followed on the TV screen and calibrated with a micrometer. The mobility was measured at two stationary levels, which were calculated to lie at 0.211 and 0.789 of the total depth of the chamber. A further check with human red blood cells showed a mobility of -1.3 ± 0.13 (μm/sec)/(volt/cm) in M/15 phosphate saline, which value is consistent with the literature value (143). All electrophoresis experiments were carried out at 24°C.

The cells were harvested, resuspended in TG buffer, then washed twice, resuspended in the following electrophoresis medium: For pH values from 2 to 4, glycine buffer was used; for pH values 4 to 10.5, glycyl-glycine buffer was used. For pH values from 2 to 6, three kinds of suspension media were employed. (a) plain 0.01 M buffer, (b) 0.01 M buffer with 0.02 N KCl, and (c) 0.01 M buffer with 0.02 N KCl plus solution T which had the following composition 1.5 mM $(NH_4)_2SO_4$, 4.2 mM $MgSO_4.7H_2O$ and 1.7 mM $CaCl_2.2H_2O$. For studies dealing with pH 6 to

10.5, only the third kind of suspension medium was employed. To investigate the dependence of mobility on the Ca^{++} and K^{+} ion concentrations, electrophoresis was performed with 0.01 M glycine buffer at pH 2, and 0.01 M glycyl-glycine buffer at pH 6, over a concentration range varying from 10^{-5} N to 0.1N of the cation concentration.

Results

Membrane Potential Calculated by the Distribution of SCN^{-}

The SCN^{-} anion was accumulated in the cells whereas the TEA^{+} cation was not accumulated in the cells. This demonstrates that the cells are charged positively inside. The membrane potential Ψ lies between 109 and 125 mV, (positive inside) (Table 3). Because Ψ is a logarithm of a ratio, the variation within each set of experiments is small, at most 3 to 5 mV, but variations between different sets of experiments may be larger. This may arise from the error made when estimating the intracellular water space; e.g., a 100 percent error causes only 10 percent change in the calculated membrane potential.

Validity of Using SCN^{-} Distribution Method to Measure Membrane Potential

In order that the ratio $[SCN^{-}]_{in}/[SCN^{-}]_{out}$ truly reports the membrane potential, the following conditions must be fulfilled: (1) KSCN should be mostly in the ionized form, (2) SCN^{-} is passively permeable to the cell membrane, in the sense that no substrate specific active accumulation of SCN^{-} into the cell take place, (3) the SCN^{-} concnetration should be small enough such that the SCN^{-} itself does not perturb the membrane potential. On the other hand, a high external SCN^{-}

Table 3

Determination of the membrane potential in Thermoplasma acidophila by measuring the distribution of radioactive $S^{14}CN^-$ across the plasma membrane.*

V_t is the total pellet water space. V_e is the extracellular pellet water space.
$V_i = V_t - V_e$ is the intracellular water space.

The membrane potential was calculated from

$$\Psi = \frac{RT}{F} \ln \frac{[SCN^-]_{in}}{[SCN^-]_{out}} = 65 \frac{[SCN^-]_{in}}{[SCN^-]_{out}}$$

where the anion concentration $[SCN^-]_{in}$ was calculated from eq. (1).

*All experiments were done at 56°C and pH 2. Influence of high KSCN concentrations and inhibitors upon the membrane potential were measured parallel to the control from the same cell batch. Expt. 1 to 3 were from different batches. Expt. 1 to 3 and all the controls represent the variations between the batches. C_s and C_p represent typical data of a single tube selected from a group of 8 tubes.

Table 3 (cont'd.)

	Expt. 1	Expt. 2	Expt. 3	Control	0.01N KSCN	0.1N KSCN	Control	10 mM NaN_3	Control	1 mM 2,4-DNP	Control	5 mM CCCP
C_s(dextran-^{14}C),cpmx10^3	86.6	34.2	85.0	79.9	76.5	93.1	93.9	92.2	85.1	89.0	76.2	84.1
C_p(dextran-^{14}C),cpmx10^3	2.22	1.13	2.33	2.28	2.12	2.21	1.99	1.89	2.08	2.12	1.18	1.18
V_t,µl	63±1	100±2	68±1	74±1	74±1	65±2	53±1	52±1	61±1	59±1	36±1	34±1
V_e,µl	54±3	73±4	58±3	60±5	58±5	50±3	44±3	43±3	51±4	50±4	33±1	30±1
V_i,µl	9±4	27±6	10±4	14±6	16±6	15±5	9±4	9±4	10±5	9±5	3±2	4±2
C_s(KS^{14}CN),cpmx10^3	39.2	52.1	57.5	54.8	63.4	104.	39.5	56.0	27.7	31.0	69.4	49.0
C_p(KS^{14}CN),cpmx10^3	15.3	38.3	22.0	18.1	11.9	7.4	10.9	11.2	8.7	9.4	10.0	9.7
$[SCN^-]_{in}/[SCN^-]_{out}$	86±10	57±4	70±4	46±5	22±2	7±1	53±8	46±3	61±7	65±8	70±9	79±12
Ψ, mV	125±5	114±2	120±2	109±2	88±3	54±4	112±4	108±2	116±3	117±3	118±5	112±5

concentration should depress the observed potential, because it is lowered by any passively permeant anion present at high concentrations.

Because HSCN is a rather strong acid with a pK = -1.85 (144). At pH 2, more than 99% of SCN^- should be in the ionized form. To test whether the SCN^- anion passively permeates the cell membrane, two kinds of experiment were performed. First, the SCN^- accumulated inside the cell can be readily washed out by the same buffer applying three washes (Figure 17). For comparison, acetate cannot be washed out (Figure 17). Secondly, increasing the external nonradioactive KSCN concentration to 1 mM, the amount accumulated depends linearly on the KSCN concentration (Figure 18). However, upon increase of the external SCN^- concentration to 0.01 N, the membrane potential was reduced to 87 mV; upon further increase to 0.1 N, the membrane potential was lowered to 54 mV (Table 3). This behavior confirms the notion that at lower concentrations the SCN^- distribution does indeed monitor the membrane potential as we proposed.

Influence of Metabolic Inhibitors on Membrane Potential

In the presence of 10 mM NaN_3, an electron transport inhibitor, or 1 mM 2,4-dinitrophenol, or 5 mM carbonyl cyanide, m-chlorophenyl hydrazone (CCCP), which are proton conducting uncouplers, the measured membrane potential remained unchanged (Table 3). As reported previously (134), similar inhibitors exerted no measurable influence upon the intracellular pH. Therefore, both the membrane potential and the pH gradient are maintained passively. The 120 mV membrane potential, (positive inside), compensates only partially the pH gradient of 4.5 pH

Figure 17. Removal of radioactive material by washing Thermoplasma acidophila cells with suspension buffer.
X——— X KS^{14}CN. •——— • ^{14}C-labelled Acetate.
Acetate included for comparison.

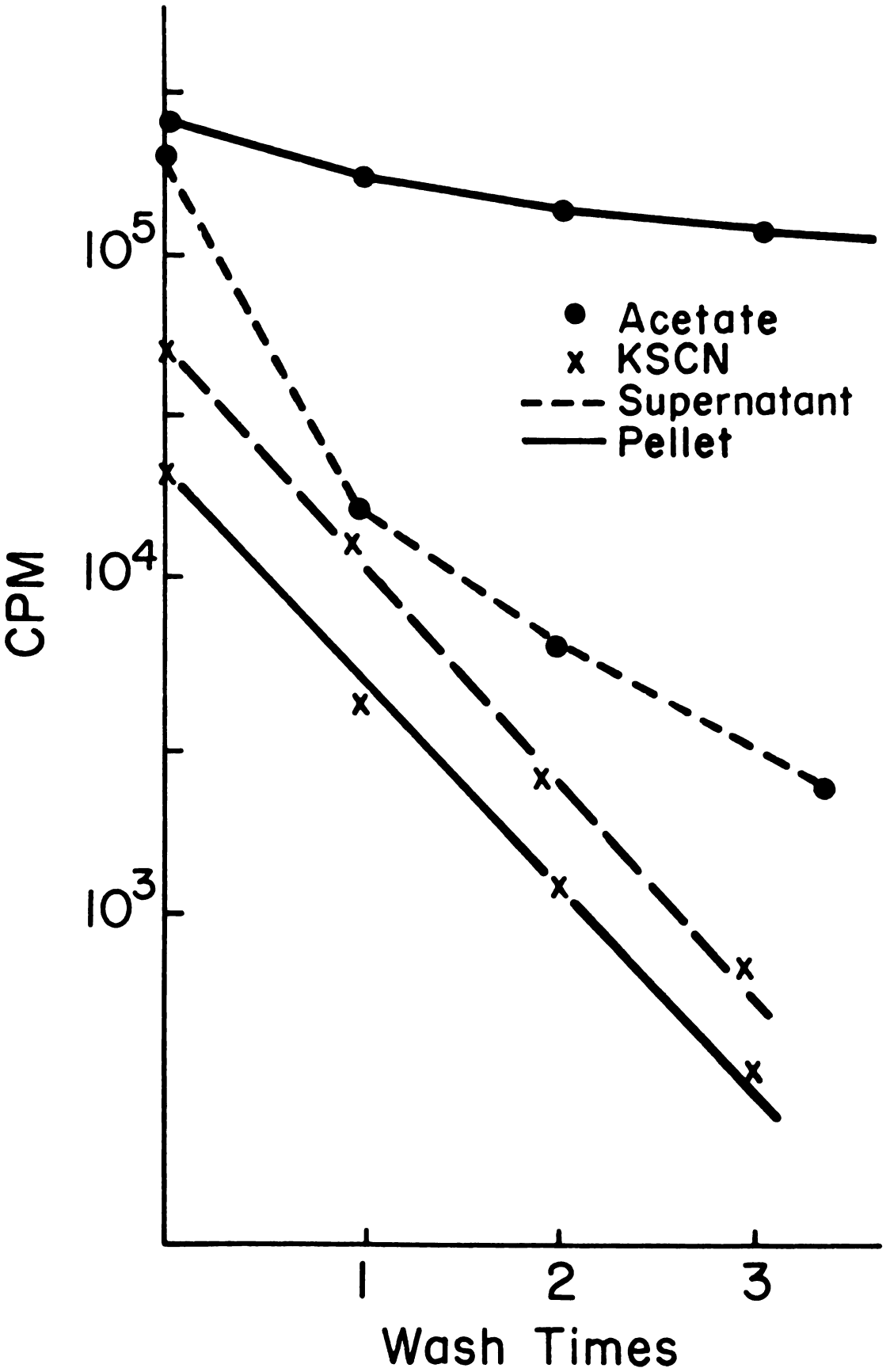
CPM
10^5
10^4
10^3
Acetate
KSCN
Supernatant
Pellet
1
2
3
Wash Times

Figure 17

Figure 18. Dependence of intracellular SCN^- concentration on the extracellular one in Thermoplasma acidophila cells.

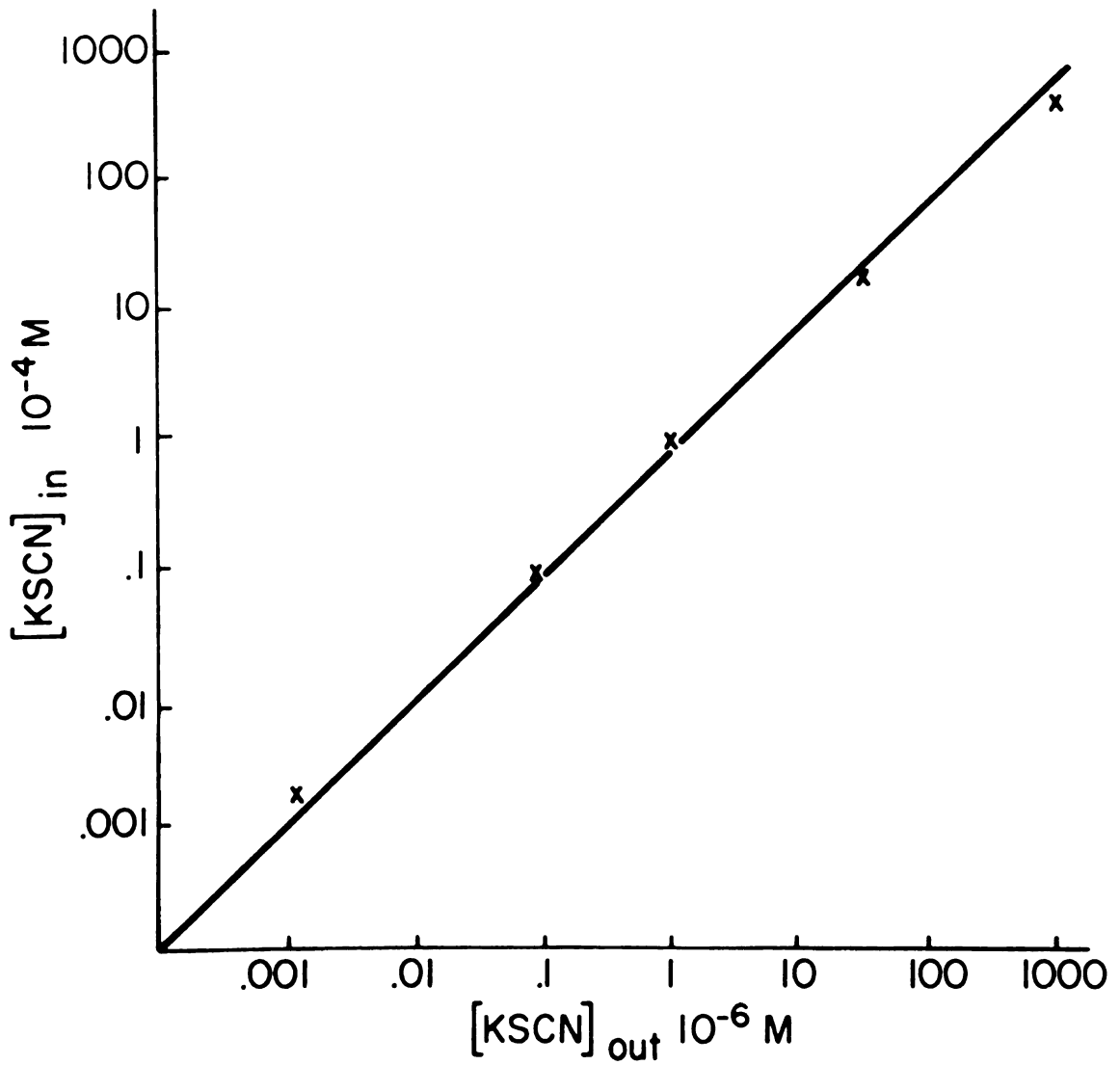
1000
100
10
1
.1
.01
.001
[KSCN]in 10-4 M
.001
.01
.1
1
10
100
1000
[KSCN]out 10-6 M

Figure 18

units, The membrane potential decreased linearly upon increase of the external pH (Figure 19). At pH 6, the potential is diminished to less than 15 mV. From Figure 19, one finds a slope of 28 mV / pH unit which is approximately one half of RT/F. We have presently no explanation for this factor of 1/2.

Electrophoretic Mobility

The Thermoplasma acidophila cells moved from the negative to the positive electrode. Thus, the net surface charge is negative, with a surface zeta-potential negative relative to the bulk of the medium. Table 4 lists the effects of different pH values, KCl and $CaCl_2$ concentrations and different ionic strengths on the electrophoretic mobility, the zeta-potential, and the surface charge density.

The mobility remained constant around u = -0.62 (μm/sec)/(volt/cm) in the pH range from pH 2 to pH 5. When the external pH was increased to pH 6.0, the mobility increased abruptly to u = -1.3 (μm/sec)/(volt/cm), followed by a steady increase as the pH became alkaline (Figure 20).

In 0.01 N glycine buffer pH 2, with 0.02 N KCl and solution T, which is close to the ionic strength and divalent cation concentrations of the growth medium, the surface charge density is 1360 esu/cm^2. This charge density corresponds to 5.7 x 10^4 elementary charges/cell, or one elementary charge / 3500 A^2 (assuming a cell with a diameter of 0.8 μm).

The effects of Ca^{++} and K^+ concentration on the mobility of the cell is shown in Figure 21. At pH 2, and at concentrations below 1 mM, both K^+ and Ca^{++} have a slight effect on the mobility of the cell. The mobility was reduced only by 50% when the cation concentration was

Figure 19. Dependence of membrane potential on the external pH of Thermoplasma acidophila cells suspended in suspension media composed of 0.02N KCl, 0.04M sucrose, solution T (1.5mM $(NH_4)_2SO_4$, 4.2mM $MgSO_4.7H_2O$ and 1.7mM $CaCl_2.2H_2O$), and 0.01N glycine buffer, for pH 2 and 3.85. For pH 5 and 6, the glycine buffer was replaced by citrate buffer.

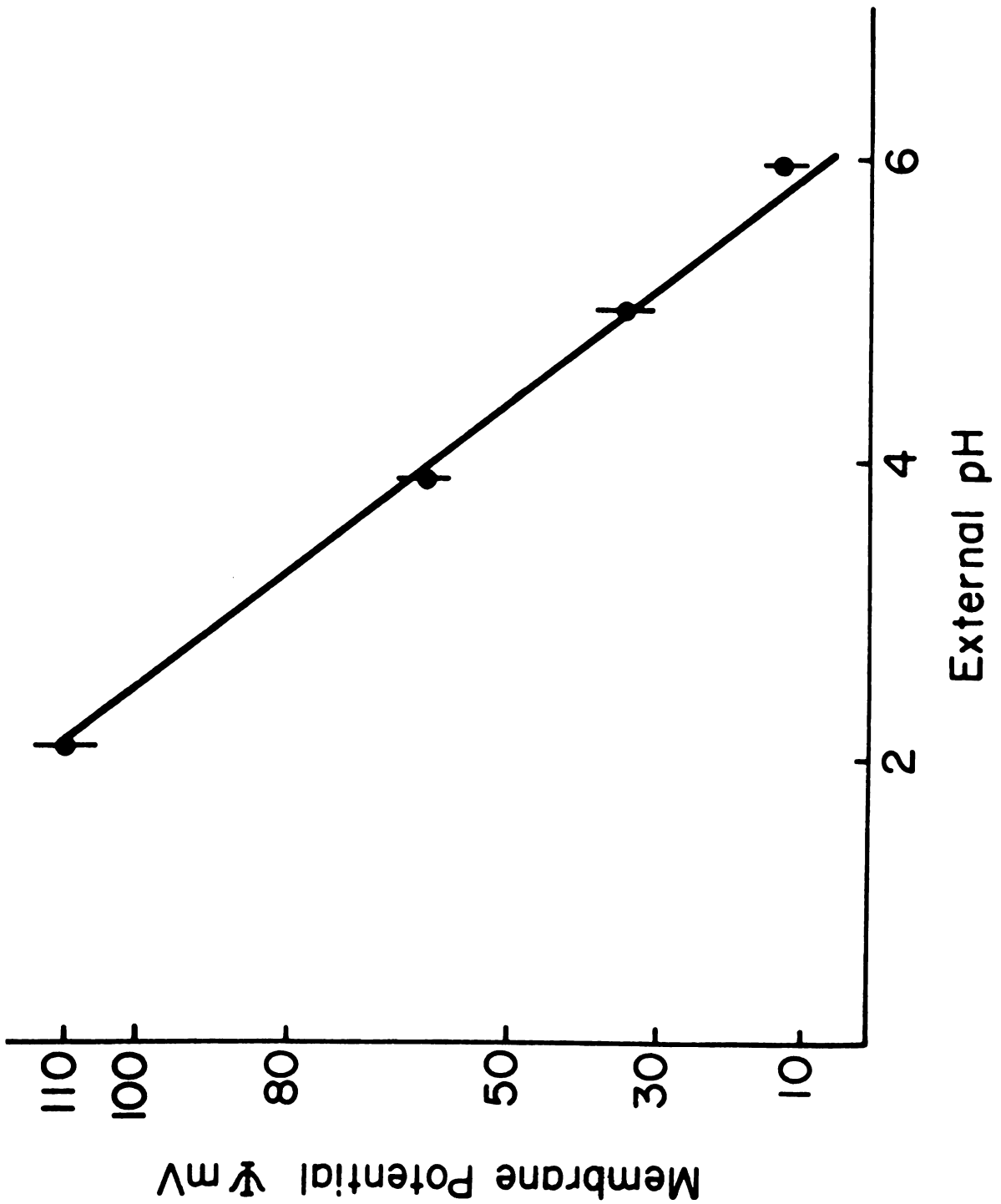

Figure 19

Table 4

The electrophoretic mobility u, zeta-potential ζ, and surface charge density σ of Thermoplasma acidophila at various pH, ionic strength, and divalent ion concentration.

	Ionic Strength	$\frac{1}{\kappa}x10^8$ cm^{-1}	$-u^*$ $\frac{(\mu m/sec)}{(volt/cm)}$	ζ^* mV	σ esu/cm^2
pH 2, plain buffer	0.01	30.3	0.936	12.3	850
pH 2, 0.02 N HCl	0.03	17.5	0.803	10.6	1260
pH 2, 0.02 N KCl Solution T**	0.056	12.8	0.635	8.3	1362
pH 6, plain buffer	0.01	30.3	2.74	36.1	2677
pH 6, 0.02 N KCl	0.03	17.5	2.24	29.4	3677
pH 6, 0.02 N KCl Solution T**	0.056	12.8	1.27	16.7	2826
pH 2, 10^{-3} N KCl	0.011	28.9	0.86	11.3	817
pH 2, 0.05 N KCl	0.06	12.4	0.47	6.2	1035
pH 2, 10^{-4} N $CaCl_2$	0.0103	29.8	0.81	10.6	743
pH 2, 10^{-3} N $CaCl_2$	0.013	26.6	0.71	9.3	745
pH 2, 10^{-2} N $CaCl_2$	0.04	15.1	0.38	5.1	718
pH 2, 0.1 N $CaCl_2$	0.31	5.44	0.35	4.6	1790
pH 6, 10^{-3} N KCl	0.011	28.9	2.5	32.9	2526
pH 6, 0.05 N KCl	0.06	9.9	2.2	29.2	5161
pH 6, 10^{-4} N $CaCl_2$	0.0103	29.9	2.4	31.6	2362
pH 6, 10^{-3} N $CaCl_2$	0.013	26.6	0.98	12.9	1042
pH 6, 0.01 N $CaCl_2$	0.04	15.2	0.47	6.2	880
pH 6, 0.1 N $CaCl_2$	0.31	5.4	0.45	5.9	2344

* The standard deviation of u and ζ is about 10% each.

**Solution T: 1.5 mM $(NH_4)_2SO_4$, 4.2 mM $MgSO_4 \cdot 7H_2O$ and 1.7 mM $CaCl_2 \cdot 2H_2O$

Figure 20. Dependence of electrophoretic mobility on pH. The suspension solution was 0.01N glycine (pH 2 to 4) or 0.01N glycyl-glycine buffer (pH 4 to 10.5), 0.02N KCl, and solution T.

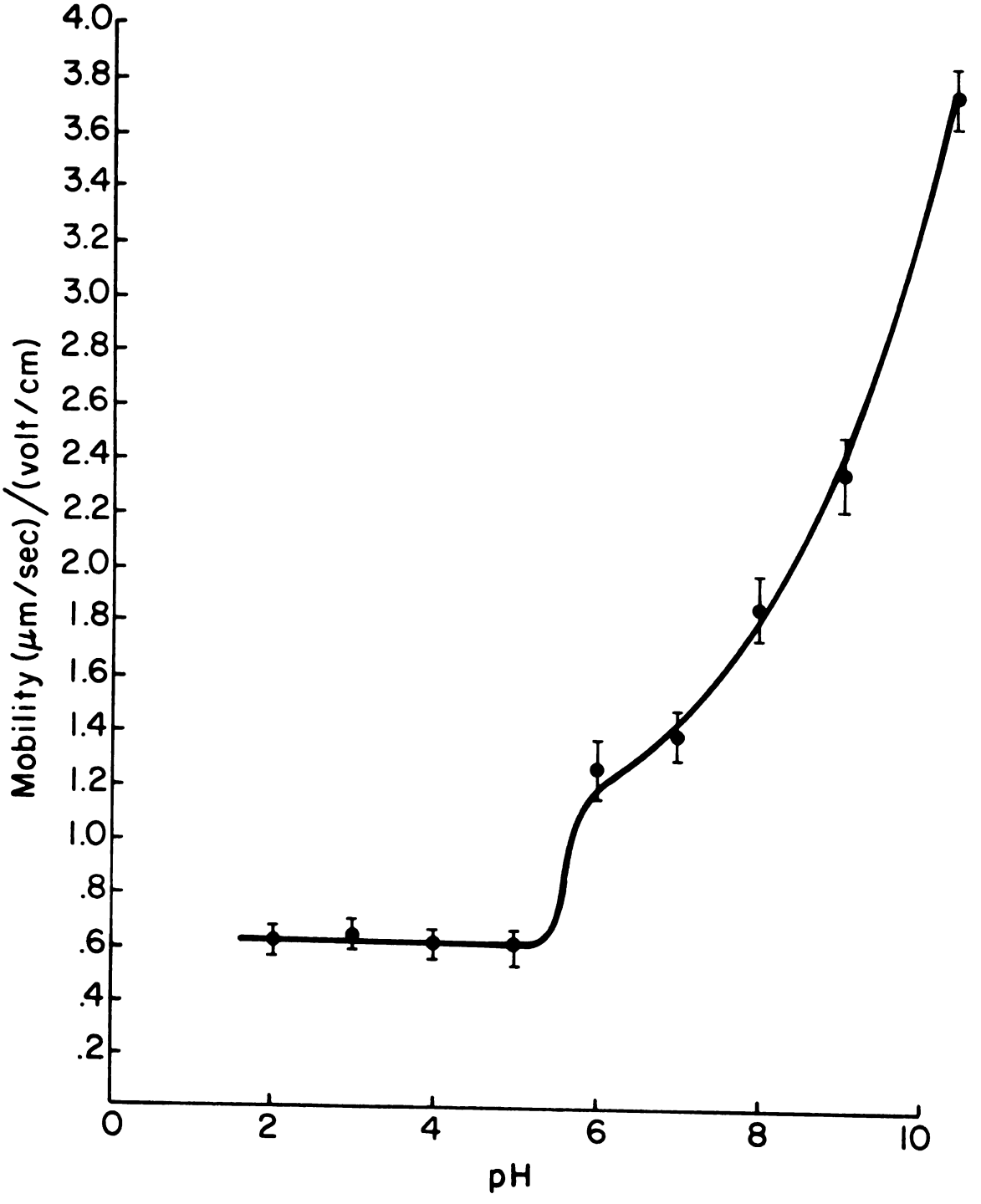
4.0
3.8
3.6
3.4
3.2
3.0
2.8
2.6
2.4
2.2
2.0
1.8
1.6
1.4
1.2
1.0
.8
.6
.4
.2
Mobility (μm/sec)/(volt/cm)
0
2
4
6
8
10
pH

Figure 20

Figure 21. Dependence of electrophoretic mobility on the cation concentrations. For pH 2, 0.01N glycine buffer, for pH 6, 0.01N glycyl-glycine buffer.

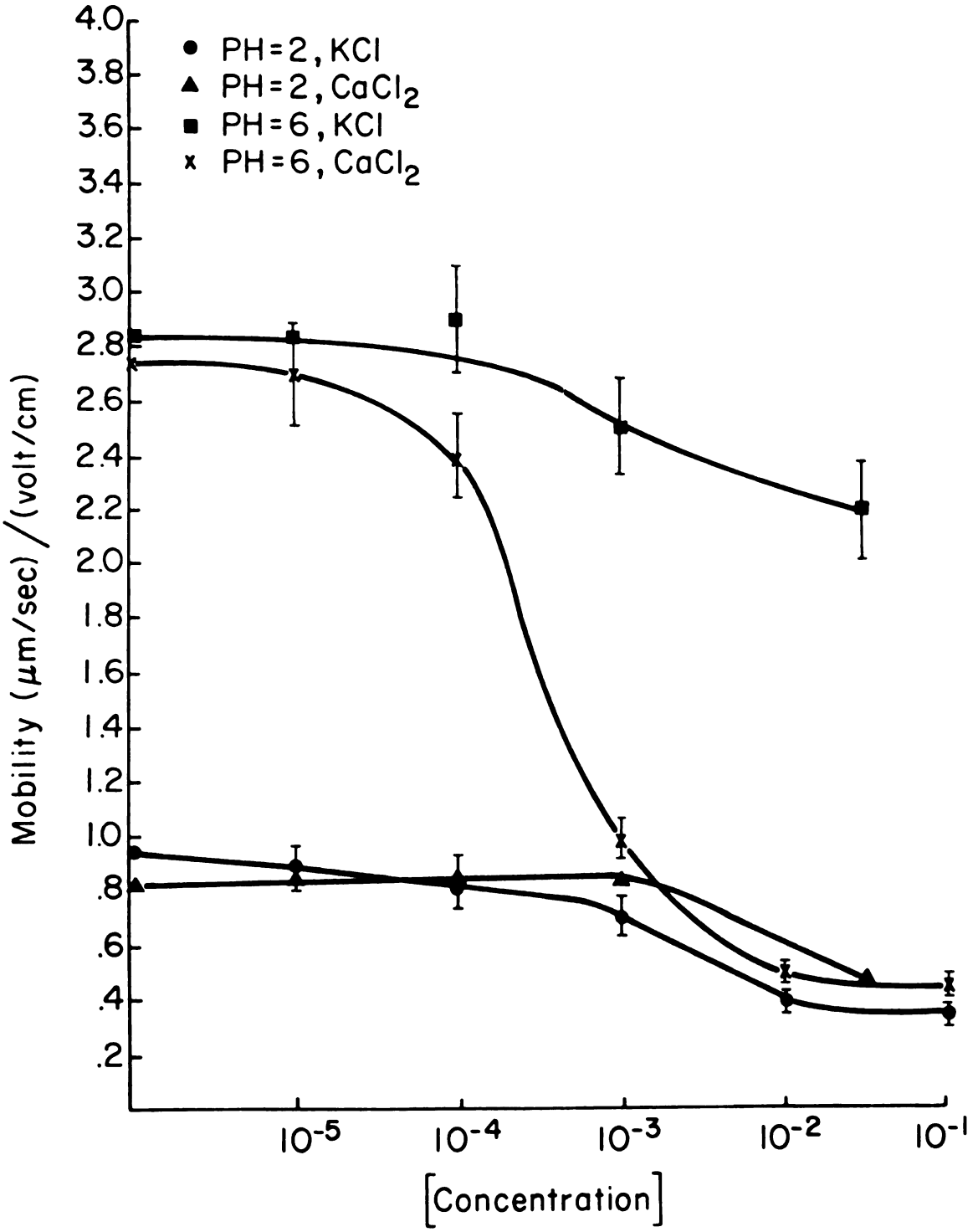
PH=2, KCl
PH=2, CaCl2
PH=6, KCl
PH=6, CaCl2
Mobility (μm/sec) / (volt/cm)
4.0
3.8
3.6
3.4
3.2
3.0
2.8
2.6
2.4
2.2
2.0
1.8
1.6
1.4
1.2
1.0
.8
.6
.4
.2
10-5
10-4
10-3
10-2
10-1
[Concentration]

Figure 21

increased to 0.01 N or 0.1 N, which is presumably an ionic strength effect. At pH 6, the effect of Ca^{++} concentration of the electrophoretic mobility of Thermoplasma acidophila cells was dramatic. The mobility had a value of -2.7 (μm/sec)/(volt/cm) when the concentration of Ca^{++} was lower than 5×10^{-5}N, and changed to -0.5 (μm/sec)/(volt/cm), i.e., a 5-fold decrease, when the Ca^{++} concentration increased to 0.01N and higher values. The Ca^{++} ion concentration which reduced the mobility to half its value was 5×10^{-4}N. At pH 6, K^{+} ions of concentrations similar to Ca^{++} concentration had little effect on the electrophoretic mobility of Thermoplasma acidophila cells.

Discussion

Based on the membrane potential measured by the method of SCN^{-} distribution, the surface charge density, and the zeta-potential estimated from electrophoretic mobility, a model for a Thermoplasma acidophila was drawn (Figure 22).

The SCN^{-} distribution measured the potential difference between the bulk phase of the cytoplasm relative to that of the external medium. The electrophoretic mobility measurement gave the surface potential difference between the outer surface of the cell and the bulk phase of the external medium.

The surface charge of Thermoplasma acidophila was inferred to be negative. This conclusion is based on several facts: (1) The cells move from the negative electrode to the positive electrode. (2) When the external pH was raised above pH 6, the mobility increased. This was presumably due to the fact that more negative charges were exposed by raising the pH, since the pK of some carboxyl groups lies around

Figure 22. A model for Thermoplasma acidophila; the surface is negatively charged, and the potential difference between two bulk phases is 120 mV (positive inside), a zeta-potential of about 8 mV exists between the external surface of shear to the bulk phase of the external medium, when the external medium is at the same pH, ionic strength and divalent ion concentrations of the growth medium.

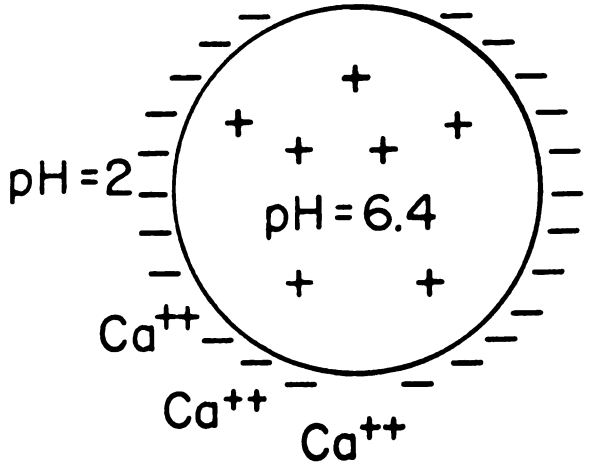
pH=2
pH=6.4
Ca++
Ca++
Ca++

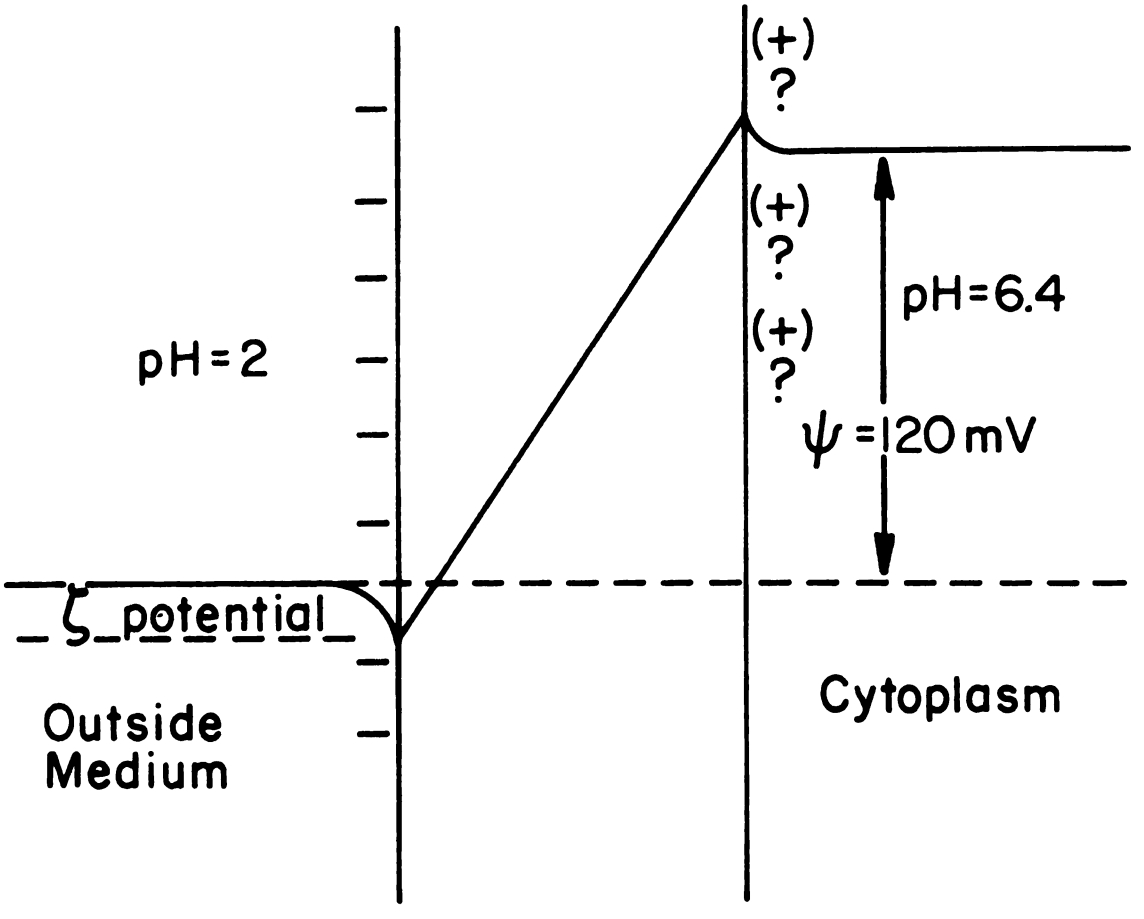
(+)
?
(+)
?
(+)
?
pH=6.4
pH=2
ψ=120mV
ζ potential
Outside
Medium
Cytoplasm
Membrane

Figure 22

4.5. (3) Ca^{++} ions, in the concentration range of 1 mM and up, reduced the electrophoretic mobility at pH 6. This effect was explained by assuming that Ca^{++} ions are specifically bound to the negatively charged cell surface, probably to the phosphate head groups of the phospholipids, since Ca^{++} has the similar binding behavior to the monolayers and bilayers of phosphatidylserine (145). We interpreted the data in terms of specific binding rather than unspecific ionic strength effects. This conclusion is based on two facts: First, KCl at concentrations of comparable ionic strength showed little effect in reducing the mobility. Secondly, the Ca^{++} ion concentration needed in reducing the mobility was rather low, viz., 5×10^{-4} N Ca^{++} ion could reduce the electrophoretic mobility to half the value measured in the absence of Ca^{++} (Table 4, and Figure 21). At pH 2, most of the binding sites are protonated, and therefore few Ca^{++} ions can be bound. It is interesting to note that at pH 6, a high Ca^{++} ion concentration (higher than 0.01 N) could reduce the mobility of Thermoplasma acidophila cells to a level found at pH 2 (Table 4, Figure 21). Thus H^{+} and Ca^{++} ions have similar and competitive effects in reducing the mobility of the cells. This interpretation of Ca^{++} binding to the cell surface is consistent with the Ca^{++} effect on the phase transition temperature of Thermoplasma acidophila membranes measured by EPR spin technique (146).

The total charge of the cell is negative, the bulk potential across the membrane is positive inside, and the surface is highly negatively charged. Therefore, inside the cell some positive ions or macromolecules may exist which cannot penetrate the cell membrane. These particles are responsible for the Donnan potential which is

positive inside the cell. We do not have any direct evidence for such an existence, but we do have some indicative evidence. From pH 7 to 10.5, the mobilities of the cells are abnormally high (Figure 20). This may be explained by cytoplasmic or membrane proteins leaking out of the cell (the proteins do leak out at pH higher than 7, see reference 135, also Figure 13, Chapter III of this dissertation). Because the mobility increased dramatically, the materials which leaked out must be positively charged.

Will the negatively charged membrane pose some problems for the anion SCN^- to penetrate into the cell? The answer is no. The question of how SCN^- permeates the negatively charged biological membrane in general and the Thermoplasma acidophila membrane in particular can be explained by the fact that the estimated charge density of various biological membranes ranges from 100 to 40 000 A^2 per elementary charge (147-150). For Thermoplasma acidophila cells, the estimated charge density ranges from 1000 to 6000 A^2 per elementary charge (Table 4). With such a low density, the charge is probably distributed discretely (150-152). Thus, there is plenty of space for SCN^- ion to diffuse through the membrane.

We do not have any information about the surface on the cytoplasmic side of the membrane. It may be positive or negative. In Figure 22 it is tentatively drawn as positive. (This is purely an assumption, made to isslutrate a point). Thus, a zeta-potential may also exist on the inner surface of the membrane. Consequently, the "real potential across the bilayer" may be 15 mV higher than the bulk-to-bulk phase potential difference measured by SCN^- distribution.

The surface zeta-potential will also influence the local pH near the surface of the membrane (153). If the cytoplasmic side of the

membrane really has a surface potential more positive than that of the bulk of the cytoplasm, the local pH near the inner surface is more alkaline than that of the bulk phase, and the local pH at the external surface is lower than that of the bulk of the medium.

The pH and Ψ profile of Thermoplasma acidophila might be important with respect to Mitchell's chemiosmotic hypothesis (this particular point, see reference 36). From kinetic experiments in chloroplasts, it was found that the H^+ current generated by light would immediately return to trigger ATP synthesis, before the H^+ to be equilibrated between the membrane solution interface and the bulk phase (154). This finding makes the zeta-potential and pH near the membrane surface an important and interesting parameter to investigate. Unfoutunately, the zeta-potential and surface charge density on the cytoplasmic side of the membrane cannot be measured by a simple direct technique.

Lastly, we would like to raise the question of whether the chemiosmotic theory of energy coupling, proposed by Mitchell (37,40,47) may be applied to this organism, i.e., can the respiratory transport of H^+ and its return to intuce ATP synthesis be the mechanism for energy transduction in Thermoplasma acidophila? At first glance, it seems that the data observed are incompatible with the Mitchell's hypothesis, since the total proton motive force needed for ATP synthesis is 270 mV (negative inside) (54,75,79). However, even at pH 2, the net electrochemical potential gradient in the resting state of the cell is -170 mV (negative inside), (-290 mV from pH gradient, +120 mV from Donnan potential).

We do not consider these data as incompatible with the Mitchell hypothesis, because the -270 mV required should be the proton electrochemical potential gradient of a respiring energized cell. Our -170 mV was obtained from resting cells.

This observation of course does not provide any direct evidence which supports the chemiosmotic theory either. However, we do have some indirect hints that the chemiosmotic theory may still be applied to this organism. In Thermoplasma acidophila, the cell polarity is reversed in comparison to Escherichia coli cells or mitochondria, either of them is negative inside. Thermoplasma acidophila constantly faces a very acidic environment, and consequently a huge hydrogen ion concentration gradient, normally not faced by other organisms. In the absence of a passive Donnan potential, Thermoplasma acidophila would then need a special kind of respiratory chain which would eject H^+ against an abnormally high electrochemical potential barrier. The reversible H^+ ion transporting ATPase would also face an abnormal high electrochemical potential barrier.

Therefore, Thermoplasma acidophila, using a passive Donnan potential (positive inside) to reverse its cell polarity, could partially balance the huge pH gradient. In this way, the remaining electrochemical potential barrier for both respiratory proton transport and the reversible proton transporting ATPase is of the same order of magnitude usually found in Escherichia coli or mitochondria. This aspect suggests that the Mitchell hypothesis may still be applicable for Thermoplasma acidophila. Nevertheless, Mitchell's hypothesis offers an explanation for the fact that Thermoplasma acidophila cells do not grow above pH 4.5, since at this pH value the membrane potential ψ drops to +40 mV. Consequently, $|\psi - (RT/F) \ln (\Delta pH)|$ (negative inside) becomes less than 80 mV. This makes the coupling mechanism of oxidative phosphorylation non-functional. Thus. the cell is likely to be not just shielded passively from the acidic environment.

BIBLIOGRAPHY

BIBLIOGRAPHY

1. Schrödinger, E. (1944) "What is life", Cambridge University Press, London and New York.

2. Kaback, H.R. (1972) Biochim. Biophys. Acta 265, 367.

3. Roseman, S. (1972) In "The Molecular Basis of Biological Transport", (Woessner, J.F. and Huining, F. eds.) p. 181, Academic Press, New York and London.

4. Boos, W. (1974) Annu. Review of Biochemistry 43, 123.

5. Azzone, G.F., Carafoli, E., Lehninger, A.L., Quagliariello, E. and Siliprandi, N. (eds.) (1972) "Biochemistry and Biophysics of Mitochondrial Membranes", Academic Press, New York and London.

6. Avery J. (ed.) (1973) "Membrane Structure and Mechanisms of Biological Energy Transduction". Plenum Press, London and New York.

7. Osborn, M.J. (1971) In "Structure and Function of Biological Membranes" (Rothfield, L.I. ed.) p. 343, Academic Press, New York.

8. Brock, T. (1967) Science 158, 1012.

9. Davson, H., and Danielli, J.F. (1952) "The Permeability of Natural Membranes". 2nd ed., Cambridge University Press, London and New York.

10. Robertson, J.D. (1964) In "Cellular Membranes in Development", (Locke, M. ed.), p. 1, Academic Press, New York and London.

11. Gorter, E. and Grendel, F. (1925) J. Expt. Med. 41, 439.

12. Zwaal, R.F.A., Demel, R.A., Roelofsen, B. and van Deenen, L.L.M. (1976) TIBS 1, 112.

13. Mueller, P., Rudin, D.O., Tien, H.T. and Wescott, W.C. (1962) Nature 194, 979.

14. Tien, H.T. (1974) "Bilayer Lipid Membrane (BLM). Theory and Practice", Marcel Dekker, Inc. New York.

15. Singer, S.J. (1971) In "Structure and Function of Biological Membranes" (Rothfield, L.I. ed.) p. 145, Academic Press, New York and London.

16. Singer, S.J. and Nicolson, G.L. (1972) Science 175, 720.

17. Bayer, M.E. and Remsen, C.C. (1971) J. Bacteriol. 101, 304.

18. Branton, D. (1969) Annu. Review of Plant Physiology 20, 209.

19. Bretscher, M.S. (1973) Science 181, 622.

20. Phillips, D.R. and Morrison, M. (1970) Biochem. Biophys. Research Communications 40, 284.

21. Lee, A.G. (1975) Progress in Biophys. and Mol. Biol. 29, (Butler, J.A.V. and Noble, D. eds.) p.5, Pergamon Press, Oxford and New York.

22. Chapman, D. (1975) Quart. Review of Biophys. 8, 185.

23. Levine, Y.K. (1973) In "Progress in Surface Science" Vol 3, (Davison, S.G. ed.) Pergamon Press, Oxford.

24. Steim, J.M., Tourtellotte, M.E., Reinert, J.C., McElhaney, R.N. and Rader, R.L. (1969) Proc. Nat. Acad. Sci. U.S. 63, 104.

25. Azzi, A. (1975) Quart. Review of Biophys. 8, 237.

26. McConnell, H.M. and McFarland, B.G. (1970) Quart. Review of Biophys. 3, 91.

27. Berliner, L.J. (1976) "Spin Labelling, Theory and Applications", Academic Press, New York and London.

28. Razin, S. (1969) Annu. Review of Microbiol. 23, 317.

29. Maniloff, J. and Morowitz, H.J. (1972) Bacteriol. Review 36, 263.

30. Smith, P.E. (1971) "The Biology of Mycoplasma", Academic Press, New York and London.

31. Rottem, S. and Razin, S. (1967) J. Bacteriol. 94, 359.

32. Razin, S. (1968) J. Bacteriol. 96, 687.

33. Razin, S., Morowitz, H.J. and Terry T.M. (1965) Proc. Nat. Acad. Sci. U.S. 54, 219.

34. Razin, S. (1972) Biochim. Biophys. Acta 265, 241.

35. Slater, E.C. (1953) Nature 172, 975.

36. Slater, E.C. (1971) Quart. Review of Biophys. 4, 35.

37. Mitchell, P. (1961) Nature 191, 144.

38. Mitchell, P. (1966) Biol. Review of Cambridge Phiol Soc. 41, 445.

39. Mitchell, P. (1966) "Chemiosmotic Coupling in Oxidative and Photosynthetic Phosphorylation", Glynn Research Ltd., Bodmin, Cornwall, England.

40. Mitchell, P. (1968) "Chemiosmotic Coupling and Energy Transduction", Glynn Research Ltd., Bodmin, Cornwall, England.

41. Boyer, P.D. (1965) In "Oxidases and Related Redox Systems", Vol. II (King, T.E., Mason, H.S. and Morrison, M. eds.) p. 994, Wiley, New York and London.

42. Green, D.E. and Harris, R.A. (1969) FEBS Letters 5, 241.

43. Harris, R.A., Penniston, J.T., Asai, J. and Green, E.E. (1968) Proc. Natl. Acad. Sci. U.S. 59, 830.

44. Greville, G.D. (1969) Current Topics of Bioenergetics 3, 1.

45. Slater, E.C. (1966) In "Regulation of Metabolic Process in Mitochondria", (Tager, J.M., Papa, S., Quagliariello, E. and Slater, E.C. eds.) p. 541, Elsevier, Amsterdam.

46. Boyer, P.D. (1968) In "Biological Oxidations", (Singer, T.P. ed.) p. 193, Wiley (Interscience) New York.

47. Green, D.E. and Ji, S. (1972) J. Bioenergetics 3, 159.

48. Green, D.E. (1974) Biochim. Biophys. Acta 346, 27.

49. Blondin, G.A. and Green, D.E. (1975) Chemical and Engin. News 10, 26.

50. Pressman, B.C. (1972) In "Biochemistry and Biophysics of Mitochondrial Membranes" (Azzone, G.F., Carafoli, E., Lehninger, A.L., Quagliariello, E. and Siliprandi, N., eds.), p. 591, Academic Press, New York and London.

51. Mitchell, P. (1972) J. Bioenergetics 3, 5.

52. Skulachev, V.P. (1971) Current Topics in Bioenergetics 4, 127.

53. Harold, F.M. (1972) Bacteriol. Review 36, 172.

54. Skulachev, V.P. (1972) J. Bioenergetics 3, 25.

55. Papa, S. (1976) Biochim. Biophys. Acta 456, 39.

56. Mitchell, P. and Moyle, J. (1967) Biochem. J. 105, 1147.

57. Mitchell, P. and Moyle, J. (1968) Eur. J. Biochem. 4, 530.

58. Moyle, J. and Mitchell, P. (1973) FEBS Letters 30, 317.

59. Papa, S., Guerrieri, F. and Lorusso, M. (1974) In "Dynamics of Energy-Transducing Membranes", (Ernster, L., Estabrook, R.W. and Slater, E.C., eds.) p. 417, Elsevier Publishing Co., Amsterdam.

60. Hinkle, P.C., Kim, J.J. and Racker, E. (1972) J. Biol. Chem. 247, 1338.

61. Kagawa, Y. (1972) Biochim. Biophys. Acta 265, 297.

62. Jasaitis, A.A., Nemecek, I.B., Severina, I.I., Skulachev, V.P. and Smirnova, S.M. (1972) Biochim. Biophys. Acta 275, 485.

63. Hindle, P.C. (1976) In "Mitochondria-Bioenergetics, Biogenesis and Membrane Structure", (Packer, L. and Gomez-Puyou, A., eds.) p. 183, Academic Press, New York, San Francisco and London.

64. Thayer, W.S. and Hinkle, P.C. (1975) J. Biol. Chem. 250, 5336.

65. Lehninger, A.L., Carafoli, E. and Rossi, C.S. (1967) Adv. in Enzymol. 29, 259.

66. Klingenberg, M. (1970) In "Essays in Biochemistry", (Campbell, P.N. and Kickens, F., eds.) Vol. 6, p. 119, Academic Press, London.

67. Papa, S., Guerrieri, F., Simone, S., Lorusso, M. and Larosa, D. (1973) Biochim. Biophys. Acta 292, 20.

68. Guerrieri, F., Lorusso, M., Pansini, A., Ferrarese, V. and Papa, S. (1976) J. Bioenergetics and Biomembranes 8, 131.

69. Racker, E. (1974) In "Dynamics of Energy-Transducing Membranes", (Ernster, L., Estabrook, R.W. and Slater, E.C., eds.) p. 269, Elsevier Publishing Co., Amsterdam.

70. Mitchell, P. and Moyle, J. (1967) Biochem. J. 104, 588.

71. Montal, M., Chance, B. and Lee, C.P. (1970) J. Membrane Biol. 2, 201.

72. Mitchell, P. (1972) In "Mitochondria/Biomembrane", Proc. 8th FEBS Meeting, Amsterdam , (Van Den Bergh, S.G., Borst, P., van Deenen, L.L.M., Reimersma, J.C., Slater, E.C. and Tager, J.M., eds.), Vol. 28 p. 353, North Holland-American Elsevier, Amsterdam.

73. Liberman, E.A., Topaly, V.P., Tsofina, L.M., Jasaitis, A. and Skulachev, V.P. (1969) Nature 222, 1076.

74. Hinkel, P.C. and Horstman, L.L. (1971) J. Biol. Chem. 246, 6024.

75. Mitchell, P. and Moyle, J. (1969) Eur. J. Biochem. 7, 471.

76. Bakeeva, L.E., Grinius, L.L., Jasaitis, A.A., Kuliene, V.V., Levitsky, D.O., Liberman, E.A., Severina, I.I. and Skulachev, V.P. (1970) Biochim. Biophys. Acta 216, 13.

77. Liberman, E.A. and Skulachev, V.P. (1970) Biochim. Biophys. Acta 216, 30.

78. Rottenberg, H. (1975) J. Bioenergetics 7, 61.

79. Jagendorf, A.T. and Uribe, E. (1966) Proc. Natl. Acad. Sci. U.S. 55, 170.

80. Cockrell, R.S., Harris, E.J. and Pressman, B.C. (1967) Nature 215, 1487.

81. Racker, E. (1970) Essays in Biochemistry 6, 1.

82. Senior, A.E. (1973) Biochim. Biophys. Acta 301, 249.

83. Nicholas, P. (1974) Biochim. Biophys. Acta 346, 261.

84. Schneider, D.L., Kagawa, Y. and Racker, E. (1972) J. Biol. Chem. 247, 4074.

85. Mitchell, P. and Moyer, J. (1970) In "Electron Transport and Energy Conservation (Tager, J.M., Papa, S., Quagliariello, E. and Slater, E.C., eds.), p. 575, Adriatica Editrice, Bari.

86. Darland, G., Brock, T., Samsonoff, W. and Conti, S. (1970) Science 170, 1416.

87. Brock, T. and Darland, G. (1970) Science 169, 1316.

88. Rothfield, L. and Finkelstein, A. (1968) Annu. Review of Biochemistry 37, 463.

89. Coleman, R. (1972) Biochim. Biophys. Acta 300, 1.

90. Razin, S., Tourtellotte, M.E., McElhaney, R.N. and Pollack, J.D. (1966) J. Bacteriol. 91, 609.

91. Silbert, D.F. and Vagelos, P.R. (1967) Proc. Natl. Acad. Sci. U.S. 58, 1579.

92. Sinensky, M. (1971) J. Bacteriol. 106, 449.

93. McElhaney, R.N. and Tourtellotte, M.E. (1969) Science 164, 433.

94. Rottem, S. and Razin, S. (1966) J. Bacteriol. 92, 714.

95. Mavis, R.D. and Vagelos, P.R. (1972) J. Biol. Chem. 247, 652.

96. Mavis, R.D. and Vagelos, P.R. (1972) J. Biol. Chem. 247, 2835.

97. Dedruyff, B., Van Dijck, P.W.M., Goldbach, R.W., Demel, R.A. and van Deenen, L.L.M. (1973) Biochim. Biophys. Acta 330, 269.

98. Engelman, D.M. (1971) J. Mol. Biol. 58, 153.

99. Hubbell, W.L., and McConnell, H.M. (1971) J. Am. Chem. Soci. 93, 314.

100. Tourtellotte, M.E., Branton, D. and Keith, A. (1971) Proc. Natl. Acad. Sci. U.S. 66, 909.

101. James, R. and Branton, D. (1971) Biochim. Biophys. Acta 233, 504.

102. James, R. and Branton, D. (1973) Biochim. Biophys. Acta 323, 378.

103. Kumamoto, J., Raison, J.K. and Lyons, J.M. (1971) J. Theor 131, 47.

104. Overath, P. and Traüble, H. (1973) Biochemistry 12, 2625.

105. Overath, P., Thilo, L. and Traüble, H. (1976) TIBS 1, 186.

106. Huang, L., Jaquet, D.D. and Haug, A. (1974) Canad. J. Biochem. 52, 483.

107. Henrikson, C.V. and Panos, C. (1969) Biochemistry 8, 646.

108. Chen, F.R. (1967) J. Biol. Chem. 242, 173.

109. Pollack, J.D., Razin, S., Pollack, M.E. and Cleverdon, R.C. (1965) Life Science 4, 973.

110. Rathbun, W.B. and Betlach, M.V. (1969) Anal. Biochem. 28, 436.

111. Lowry, O.H., Rosebrough, N.J., Farr, A.L. and Randall, R.J. (1951) J. Biol. Chem. 193, 265.

112. Folch, J., Lee, M. and Sloane-Staney, G.H. (1957) J. Biol. Chem. 266, 497.

113. Ne'eman, Z., Kahane, I., Kovartovsky, J. and Razin, S. (1972) Biochim. Biophys. Acta 266, 255.

114. Keith, A.D., Sharnoff, M. and Cohn, G.E. (1973) Biochim. Biophys. Acta 300, 379.

115. Raison, J.K., Lyons, J.M., Mehlhorn, R.J. and Keith, A.D. (1971) J. Biol. Chem. 246, 4036.

116. McConnell, H.M., Devaux, P. and Scandella, C. (1972) In "Membrane Research" (Fox, C.F. ed.) p. 27, Academic Press, New York.

117. Razin, S., Consenza, B.J., and Tourtellotte, M.E. (1966) J. General Microbiol. 42, 139.

118. Huang, L. and Haug, A. (1974) Biochim. Biophys. Acta 352, 361.

119. Sinensky, M. (1974) Proc. Natl. Acad. Sci. U.S. 71, 522.

120. Huang, L., Lorch, S.K., Smith, G.G. and Haug, A. (1974) FEBS Letters 43, 1.

121. Oldfield, E. and Chapman, D. (1972) FEBS Letters 23, 285.

122. Butler, K.W. (1974) Fed. Proc. 33, 1327.

123. Ruwart, M.J. (1974) "Membrane Properties of Thermoplasma acidophia" Ph. D. Thesis, Michigan State University.

124. Waddell, W.J. and Butler, T.C. (1959) J. Clin. Invest. 38, 720.

125. Addanki, S., Cahill, F.D. and Sotos, J.F. (1968) J. Biol. Chem. 243, 2337.

126. Harold, F.M., Pavlosova, E. and Baarda, J.R. (1970) Biochim. Biophys. Acta 196, 235.

127. Riebeling, V., Thaer, R.K. and Jungermann, K. (1975) Eur. J. Biochem. 55, 445.

128. Padan, E., Zilberstein, D. and Rottenberg, H. (1976) Eur. J. Biochem. 63, 533.

129. Ruwart, M.J. and Haug, A. (1975) Biochemistry 14, 860.

130. Yang, N.S. (1974) "Biochemical and Developmental Studies of the Genetically Determined MDH Isozymes in Maize", Ph.D. Thesis, Michigan State University.

131. Yang, N.S. and Scandalios, J.G. (1974) Arch. Biochem. Biophys. 161, 335.

132. McReynolds, M.S. and Kitto, G.B. (1970) Biochim. Biophys. Acta 198, 165.

133. Kitto, G.B. and Kaplan, N.O. (1966) Biochemistry 5, 3966.

134. Hsung, J.C. and Haug, A. (1975) Biochim. Biophys. Acta 389, 477.

135. Lee, C.P. (1971) Biochemistry 10, 4375.

136. Gromet-Elhanan, Z. (1972) Biochim. Biophys. Acta 275, 125.

137. Abramson, H.A. (1934) "Electrokinetic Phenomena", Reinhold, New York.

138. Briton, Jr., C.C. and Lauffer, M.A. (1959) In "Electrophoresis", (Bier, M. ed.) p. 427, Academic Press, New York.

139. Mehrishi, J.N. (1972) Progress in Biophys. and Mol. Biol. 25, (Butler, J.A.V. and Noble, D., eds.) p.1, Pergamon Press, Oxford and London.

140. Henry, D.C. (1931) Proc. Roy. Soc. A 133, 106.

141. Overbeek, J. Th. G. (1950) Advances in Colloid Sci. 3, 97.

142. Abramson, H.A., Moyer, L.S. and Gorin, M.H. (1942) "Electrophoresis of Proteins and the Chemistry of Cell Surface", Reinhold and New York.

143. Furchgott, R.F. and Ponder, E. (1941) J. Gen. Physiol. 24, 447.

144. Morgan, T.D.B., Stedman, G. and Whincup, P.A.E. (1965) J. Chem. Soc. 4813.

145. Hauser, H., Darke, A. and Phillips, M.C. (1976) Eur. J. Biochem. 62, 335.

146. Weller, Jr., H.G. and Haug, A. (1977) J. Gen. Microbiol. in press.

147. Elul, R. (1967) J. Physiol. 189, 351.

148. Segal, J.R. (1968) Biophysical J. 8, 470.

149. Rojas, E. and Atwater, I. (1968) J. Gen. Physiol. 51, 131s.

150. Nelson, A.P. and McQuarrie, D.A. (1975) J. Theor. Biol. 55, 13.

151. Cole, K.D. (1969) Biophysical J. 9, 465.

152. Brown, Jr., R.H. (1974) Progress in Biophys. and Mol. Biol. 28, (Butler, J.A.V. and Noble, D., eds.) p.343, Pergamon Press, Oxford and London.

153. Buysman, J.R. (1973) J. Theor. Biol. 38, 51.

154. Ort, D.R., Dilley, R. and Good, N.E. (1976) Biochim. Biophys. Acta 449, 108.